LADCO | LAKE MICHIGAN AIR DIRECTORS CONSORTIUM

Weather Research Forecast 2022 Meteorological Model Simulation and Evaluation

Technical Support Document

Prepared by:

Tsengel Nergui and **Zac Adelman**

Lake Michigan Air Directors Consortium

December 1, 2024

This page is intentionally left blank

Contents

Figures

Tables

.

Executive Summary

The Lake Michigan Air Directors Consortium (LADCO) prepared this technical report to document the evaluation of a 2022 Weather Research Forecast (WRF) model simulation to support regulatory air quality modeling for ozone (O_3), fine particulate matter ($PM_{2.5}$), and regional haze planning. This report details the WRF modeling inputs and configuration, modeling procedures, model evaluation methodology, and model performance analysis results. LADCO used the WRF version 4.5 model (Advanced Research WRF dynamic core WRF-ARW) to simulate meteorology on 12-km, 4-km, and 1.33-km domains focused on the Great Lakes Basin for the year 2022. The configuration of the final 2022 WRF simulation was based on results from a series of model configuration experiments completed by LADCO.

LADCO conducted qualitative and quantitative analysis to assess operational performance of the 2022 WRF modeling. Focus of this analysis is on the states in the LADCO region. For the 4-km domains, the WRF performance is evaluated by state; and for the 1.33 domains the performance is evaluated for the entire domain. LADCO compared modeled surface pressure, precipitation, and wind vectors against observations by season and for selected high-concentration O_3 events. We also performed a detailed analysis of the model during lake-breeze events at the shoreline monitors of Lake Michigan.

LADCO found that the 12-km and 4-km WRF simulations adequately captured the observed meso- and synoptic-scale processes during June 2022, during which observed surface O_3 and $PM_{2.5}$ were elevated due to fire smoke transport into the region. The LADCO WRF simulation represents very close approximation of the actual meteorology that occurred in 2022. While the WRF performance statistics for the 12-km and 4-km grid resolution simulations are within the acceptable performance benchmarks, the 12-km simulation has a slight cold and wet bias in the summer across much of the Eastern U.S. For the 4-km WRF simulation all the summer season metrics, with the exception of wind direction error, fall within the simple terrain model performance benchmarks; the wind direction error falls within the complex terrain benchmark. The 1.33 km WRF simulations had very good model performance with low errors for all variables

and biases near zero. Both errors and biases for temperature and specific humidity at the 12-km grid resolution are reduced by about 10% at the 4-km resolution. There was a slight degradation in model performance for the analyzed variables between the 4-km and 1.33-km resolution simulations.

Analysis of WRF performance at shoreline monitors during lake-breeze events showed that the model successfully reproduced the surface conditions. LADCO used a novel CART statistical model using data from selected surface stations on the shorelines of Lake Michigan for identifying lake-breeze days in 2022. WRF performed well predicting temperature, moisture, and winds at the shoreline monitors during lake-breeze events. The model performance is slightly better on the lake-breeze days compared to the non-lake-breeze days on shoreline of Lake Michigan. The 4-km and 1.33-km simulations had better performance simulating lake breeze conditions than the 12-km simulation.

1 Introduction

The Lake Michigan Air Directors Consortium (LADCO) used the Weather Research and Forecasting (WRF) model (Advanced Research WRF dynamic core WRF-ARW; Skamarock et al, 2008) to simulate meteorology in the Great Lakes Basin for the year 2022. WRF is a mesoscale numerical weather prediction system designed to serve both operational forecasting and atmospheric research needs. WRF contains separate modules to compute different physical processes such as surface energy budgets and soil interactions, turbulence, cloud microphysics, and atmospheric radiation. LADCO used the WRF Preprocessing System (WPS) to generate the initial and boundary conditions used by WRF, based on topographic datasets, land use information, and larger-scale atmospheric and oceanic models.

This report describes an application and performance evaluation of WRF version 4.5 to simulate 2022 meteorology on 12-km, 4-km, and 1.33-km domains focused on the Great Lakes Basin. This report describes the meteorology model configuration and input data (Section 2) used for the simulation; the model performance evaluation approach and results (Section 3); model performance for simulating lake-breeze events (Section 4); and conclusions and future work (Section 5).

2 WRF Model Configuration

This section describes the software configuration for the LADCO 2022 WRF simulation, including the version of the model, horizontal and vertical domain structures, input data sources, physical parameterization options, four-dimensional data assimilation (FDDA), and application methodology. LADCO designed the 2022 WRF simulation to estimate regional to continental scale meteorology to support emissions and air quality modeling applications for the Great Lakes region. The physics options for the LADCO WRF simulation were based on the best performing WRF configuration identified through several test configurations done in-house that build upon recent WRF simulations done across the U.S., including EPA WRF 2022 (US EPA, 2024; US EPA 2019), LADCO sensitivity modeling for 2022 (LADCO, 2024), and LADCO 2016 simulations (LADCO, 2022; LADCO, 2018).

2.1 WRF Model Version

LADCO used the publicly available version of WRF version 4.5. The WPS preprocessor programs were used to develop model inputs included GEOGRID, UNGRIB, and METGRID.

2.2 Horizontal Modeling Domain

LADCO simulated meteorology with WRF for three one-way nested domains that are based on the standard Lambert Conformal Conic (LCC) projection centered on the continental U.S.:

- US EPA 12US2 (d01): 12-km continental U.S. domain
- LADCO4 (d02): 4-km Great Lakes regional domain that contains all LADCO states, and parts of the adjacent states and Canada
- LADCO1.33west (d03): 1.33-km domain that focuses on coastal sites around Lake Michigan

Figure 1 illustrates the LADCO 2022 WRF modeling domains and their extents. Table 1 shows the map projection and grid parameters for the WRF modeling domains. The outer 12-km domain (d01) has 472 columns and 312 rows, selected to be consistent with the existing U.S. EPA 12US2 modeling domain[1]. The 4-km domain (d02) has 445 columns and 421 rows with an offset from

[1] https://www.epa.gov/sites/default/files/2020-10/documents/met_model_performance-2016_wrf.pdf

the d01 grid origin of 206 columns and 110 rows. The Lake Michigan 1.33-km domain (d03) has 328 columns and 493 rows with an offset from the 4-km grid origin of 186 columns and 144 rows.

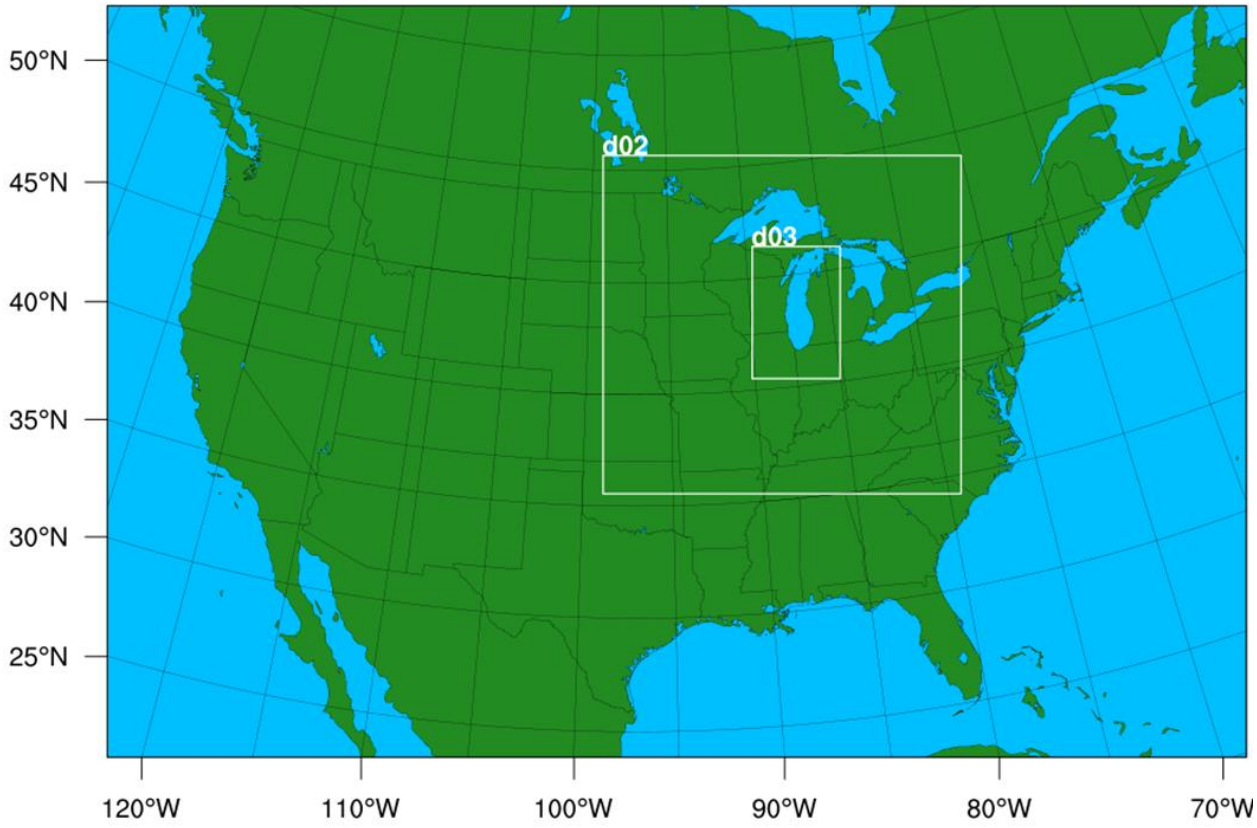

Figure 1. LADCO WRF 12/4/1.33-km domains

Table 1. Projection and grid parameters for the LADCO 2022 WRF modeling domains

Parameter	Value
Projection	Lambert-Conformal
1st True Latitude	33 degrees N
2nd True Latitude	45 degrees N
Central Longitude	-97 degrees W
Central Latitude	40 degrees N
d01 X, Y origin offset | ncol, nrow	-2412 km, -1620 km | 472, 312
d02 X, Y origin offset | ncol, nrow	-132 km, -420 km | 445, 421
d03 X, Y origin offset | ncol, nrow	576 km, 84 km | 328, 493

2.3 Vertical Layer Structure

LADCO configured the WRF model to use a terrain-following sigma coordinate system defined by pressure levels from the surface up to 50 hPa with a total of 36 vertical level interfaces (35 layers). Table 2 tabulates the LADCO WRF vertical model layer structure.

Table 2. LADCO WRF vertical layer structure

WRF Level	Height (m)	Pressure (Pa)	Sigma	Thickness (m)
36	17,556	5,000	0.000	2,776
35	14,780	9,750	0.050	1,958
34	12,822	14,500	0.100	1,540
33	11,282	19,250	0.150	1,280
32	10,002	24,000	0.200	1,101
31	8,901	28,750	0.250	969
30	7,932	33,500	0.300	868
29	7,064	38,250	0.350	789
28	6,275	43,000	0.400	722
27	5,553	47,750	0.450	668
26	4,885	52,500	0.500	621
25	4,264	57,250	0.550	581
24	3,683	62,000	0.600	547
23	3,136	66,750	0.650	517
22	2,619	71,500	0.700	393
21	2,226	75,300	0.740	285
20	1,941	78,150	0.770	276
19	1,665	81,000	0.800	180
18	1,485	82,900	0.820	177
17	1,308	84,800	0.840	174
16	1,134	86,700	0.860	170
15	964	88,600	0.880	167
14	797	90,500	0.900	83
13	714	91,450	0.910	82
12	632	92,400	0.920	81
11	551	93,350	0.930	81
10	470	94,300	0.940	80
9	390	95,250	0.950	79
8	311	96,200	0.960	79
7	232	97,150	0.970	78
6	154	98,100	0.980	39
5	115	98,575	0.985	38
4	77	99,050	0.990	39
3	38	99,525	0.995	19
2	19	99,763	0.9975	19
1	0	100,000	1.000	0

2.4 Topography and Land Use Data

LADCO developed the topographic information for WRF using standard WRF terrain databases. We based all domain simulations on nine second (~300 m) resolution topography data; the land use and land cover data were based on the 2011 National Land Cover Database. The NLCD is a 40-category, 30-meter resolution dataset of land-cover for the continental U.S.

2.5 Atmospheric Data Inputs

WRF relies on meteorological fields from other models or reanalysis (blend of model and observations) to provide initial and boundary conditions (IC/BC) and input fields for FDDA. FDDA refers to the nudging of the WRF simulation toward observed analyses to control model drift so that the WRF meteorological fields better represent actual historical conditions.

The LADCO 2022 WRF simulation used a blend of 12-km resolution North American Mesoscale Forecast System's reanalysis dataset (NAM, Grid 218) and the 3-km resolution High-Resolution Rapid Refresh Version 4 Model data (HRRRv4) for IC/BC and FDDA. The 3D NAM reanalysis data were downloaded from the NOAA's National Center for Environmental Information (NCEI) server[2] and the surface HRRRv4 dataset was accessed during September 2024 from https://registry.opendata.aws/noaa-hrrr-pds.

2.6 Diffusion Options

Horizontal Smagorinsky first-order closure with sixth-order numerical diffusion and suppressed up-gradient diffusion.

2.7 Lateral Boundary Conditions

Lateral boundary conditions were specified from a blend of the NAM and HRRRv4 initialization dataset on the 12 km CONUS domain with continuous updates nested from the 12 km domain to the 4 km domain, and continuous updates nested from the 4 km domain to the 1.33 km domain.

[2] https://www.ncei.noaa.gov/thredds/catalog/model-namanl/

2.8 Top and Bottom Boundary Conditions

The top boundary condition was selected as an implicit Rayleigh dampening for the vertical velocity. Consistent with the model application for non-idealized cases, the bottom boundary condition was selected as physical, not free slip.

2.9 FDDA Data Assimilation

LADCO constrained the WRF model solution using a combination of analysis and surface observation nudging, i.e., FDDA. We ran the WRF model with a combination of NAM and HRRRv4 analysis and observational data for 12-km and 4-km domains only. For the grid nudging we used analysis nudging coefficients of 0.3×10^{-4} s^{-1} for horizontal winds and temperature, and a coefficient of 1.0×10^{-5} s^{-1} for water vapor mixing ratio (grid_fdda). We only applied the analysis nudging above the planetary boundary layer[3]. We assimilated surface observational data in the surface grid nudging for 12-km and 4-km domains as well. The NCEP ADP Global Surface Observational Weather Data in little_r format was obtained from the Research Data Archive at the National Center for Atmospheric Research, Computational and Information Systems Laboratory (https://doi.org/10.5065/4F4P-E398, Accessed during September 2024). We applied a nudging coefficient of 0.3×10^{-4} s^{-1} for horizontal winds and temperature and a nudging coefficient of 1.0×10^{-5} s^{-1} for water vapor mixing ratio for the observation grid nudging (grid_sfdda).

2.10 WRF Physics

Version 4.5 of the WRF model, Advanced Research WRF (ARW) core (Skamarock, 2008) was used for generating the 2022 simulation. LADCO simulated winter (January 1-15) and summer (June 15-30) test periods for eight different cases of WRF configurations and found the LADCO_WRF45_APX_NAM_HRRR6_obs case was the best performing configuration with the lowest errors and biases computed at surface monitors in the LADCO region (LADCO, 2024). The LADCO WRF 2022 physics options included the Pleim-Xiu land surface model, the Asymmetric Convective Model version 2 planetary boundary layer scheme (Pleim 2007), Kain Fritsch cumulus

[3] Otte, T.L. (2008). The impact of nudging in the meteorological model for retrospective air quality simulations. Part II: Evaluating collocated meteorological and air quality observations. Journal of Applied Meteorology and Climatology, 47(7): 1868-1887.

parameterization (Kain 2004) utilizing the moisture-advection trigger (Ma and Tan, 2009), Morrison double moment microphysics (Morrison et al. 2005), and RRTMG longwave and shortwave radiation schemes (Gilliam and Pleim, 2010).

A summary of the WRF model physics and FDDA options that LADCO used for optimizing WRF performance for the Great Lakes and central Midwest U.S. are shown in Table 3.

Table 3. LADCO 2022 WRF Physics and Other Options

WRF Treatment	Option Selected	Notes
Microphysics	Thompson Scheme	mp_physics=10
Longwave Radiation	RRTMG	ra_lw_physics=4; Rapid Radiative Transfer Model (RRTM) for GCMs includes random cloud overlap and improved efficiency over RRTM.
Shortwave Radiation	RRTMG	rw_ww_physics=4; Same as above, but for shortwave radiation.
Land Surface Model (LSM)	Pleim-Xiu LSM Pleim-Xiu surface layer option	sf_surface_physics=7 sf_sfclay_physics=7
Planetary Boundary Layer (PBL) scheme	ACM2	bl_pbl_physics=7
Cumulus parameterization	Kain-Fritsch in the 12-km and 4-km domains with moisture-advection based trigger. None in the 1.33-km domain	cu_physics=1 and trigger_option=2; 1.33-km can explicitly simulate cumulus convection, so parameterization is not needed.
Analysis Nudging	Aloft nudging applied to wind, temperature, and moisture in d01 and d02	Only nudging above the planetary boundary layer
Observation in grid Nudging	Surface observation nudging applied to winds, temperature, and moisture in d01 and d02	$0.3x10^{-4}$ s^{-1} (t) $0.3x10^{-4}$ s^{-1} (uv) $1.0x10^{-5}$ s^{-1} (q)
Initialization (initial and boundary conditions)	Blend of NAM218 (12-km) with surface HRRRv4 (3-km) reanalysis data in 6-hr interval	$0.3x10^{-4}$ s^{-1} (t) $0.3x10^{-4}$ s^{-1} (uv) $1.0x10^{-5}$ s^{-1} (q)

2.11 Model Simulation Details

LADCO simulated meteorology with WRFv4.5 for the three nested domains over the U.S. on the Amazon Web Services (AWS) Elastic Compute Cloud using a distinct number of CPUs depending on pre-processing (1 node and 40 CPUs per node), actual wrf.exe simulation (4 nodes and 96 CPUs per node), and post-processing (1 node and 24 CPUs per node). The annual WRF simulation

was run in quarters. Within each quarter, WRF.exe was executed in 10-day intervals. The first 10-day block of a quarter was considered as a spin-up period with each subsequent 10-day simulation initialized with a restart file from the previous 10-day simulation, effectively simulating the quarterly WRF run continuously. We used a 60 second integration time step and the results were output at 60-minute intervals. Further, the hourly WRF results were written out to 12-hour output files (2 files/day).

LADCO simulated WRF from December 22, 2021 through February 2, 2023 for the 12-km CONUS domain (d01) and the 4-km Midwest domain (d02), and from March 21, 2022 through October 31, 2022 and for all three nested domains (d01 through d03). We successfully completed the 13-month WRF simulation on all three domains in 12 wall clock days.

3 WRF Model Performance Evaluation

LADCO conducted qualitative and quantitative analysis to assess operational performance of the 2022 WRF modeling. For the 12-km domain modeling, which covers the entire continental U.S. and parts of Canada and Mexico, we evaluated the model performance by Multi-Jurisdictional Organization (MJO) extent. MJOs are regional organizations that provide a forum for neighboring states to collaborate on air quality planning (Figure 2). The focus of this WRF performance analysis is on the LADCO region. For the 4-km domain, the WRF performance is evaluated by state; and for the 1.33 domain the performance is evaluated for the entire domain.

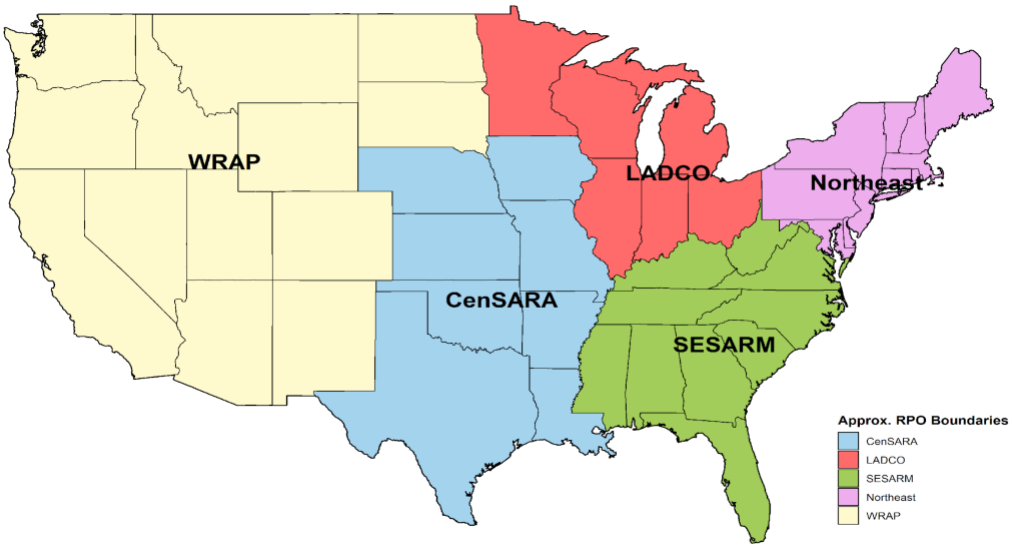

Figure 2. Multi-Jurisdictional Organizations in the Continental U.S.

LADCO conducted a standard model performance evaluation using surface observations of temperatures, winds, and humidity. We also compared modeled surface pressure, precipitation, and wind vectors against observation-based weather maps for high concentration ozone and particulate matter episodic events. Because lake-breezes are a significant dynamical feature in the region that drive some of the highest observed surface ozone concentrations, we performed a detailed analysis of model performance at Great Lakes shoreline monitors. An accurate WRF simulation of the dynamics, timing, and spatial extent of the lake-breeze is an important because it provides a base for simulating lake-breeze-driven ozone in the downstream air quality model

for the Midwest, especially for shoreline monitors adjacent to Lake Michigan. This chapter details the model performance evaluation (MPE) approach used by LADCO to understand the quality of the 2022 WRF simulation.

3.1 Model Performance Evaluation Approach

LADCO conducted qualitative and quantitative analysis to assess operational performance of the 2022 WRF modeling. The quantitative model performance evaluation of WRF using surface meteorological measurement was performed using the Atmospheric Model Evaluation Tool (AMET)[4] version 1.5. AMET calculates statistical performance metrics such as bias, error, and correlation for surface winds, temperature, and mixing ratio and can produce time series of predicted and observed meteorological variables and diurnal performance statistics.

3.1.1 Observational Data for Model Evaluation

The National Oceanic and Atmospheric Administration (NOAA) Earth System Research Laboratory (ESRL) Meteorological Assimilation Data Ingest System (MADIS) data were used to evaluate 2-m temperature, 2-m water vapor mixing ratio, and 10-m wind speed and wind direction estimates for each simulation domain and month. LADCO evaluated the WRF model hourly outputs against observed surface temperature, specific humidity, and wind fields from the METAR network. The quantitative model performance evaluation of WRF using surface meteorological measurement was performed based on collocated hourly observed and model values for grid cells in which monitors are located using the AMETv1.5 tool, and summary plots and tables were created using the statistical software R version 4.2.3.

3.1.2 Benchmarks for Meteorological Model Performance

LADCO used several performance benchmarks to evaluate the performance of the WRF 2022 simulation. Emery et al. (2001) derived and proposed a set of performance "benchmarks" for typical meteorological conditions for meteorological simulations used in air quality model applications. These performance benchmarks were based upon the evaluation of about 30 MM5 and RAMS meteorological simulations of limited duration (multi-day episodes) in support of air

[4] http://www.cmascenter.org

quality modeling study applications performed over several years. The benchmarks were based on ozone model applications for cities in the eastern and Midwestern U.S. and Texas that were primarily simple (flat) terrain and simple (stationary high-pressure and stagnant) meteorological conditions. More recently these benchmarks have been used in annual meteorological modeling studies that include areas with complex terrain and more complicated meteorological conditions; therefore, they must be viewed as being applied as guidelines and not bright-line numbers. That is, the purpose of these benchmarks is not to give a passing or failing grade to any meteorological model application, but rather to put the modeling results into the proper context of other models and meteorological data sets.

Recognizing that simple conditions benchmarks may not be appropriate for more complex conditions, McNally (2009) analyzed multiple annual runs that included complex terrain conditions and suggested an alternative set of benchmarks for temperature, namely a guideline of within ±1.0 K for bias and 3.0 K for error. As part of the Western Regional Air Partnership (WRAP) meteorological modeling of the western United States, including the Rocky Mountain Region as well as the complex conditions in Alaska, Kemball-Cook et al., (2005) proposed model performance benchmarks for complex conditions. Based on these reviews, we have adopted "simple" and "complex" model performance benchmarks for surface temperature, mixing ratio, and winds (Table 4).

Table 4. Meteorological model performance benchmarks for simple and complex conditions

Parameter	Simple	Complex
Temperature Bias	≤ ±0.5 K	≤ ±2.0 K
Temperature Error	≤ 2.0 K	≤ 3.5 K
Mixing Ratio Bias	≤ ±1.0 g/kg	NA
Mixing Ratio Error	≤ 2.0 g/kg	NA
Wind Speed Bias	≤ ±0.5 m/s	≤ ±1.5 m/s
Wind Speed RMSE	≤ 2.0 m/s	≤ 2.5 m/s
Wind Direction Bias	≤ ±10 degrees	NA
Wind Direction Error	≤ 30 degrees	≤ 55 degrees

The equations for bias, error, and root mean square error (RMSE) are given below.

$$\text{Mean Bias (Bias)} = \frac{1}{N}\sum_{i=1}^{N}(P_i - O_i)$$

$$\text{Mean Absolute Gross Error (Error)} = \frac{1}{N}\sum_{i=1}^{N}|P_i - O_i|$$

$$\text{Root Mean Square Error (RMSE)} = \left[\frac{1}{N}\sum_{i=1}^{N}(P_i - O_i)^2\right]^{1/2}$$

The following sections will present model performance results and discussion for each grid resolution.

3.2 Model Performance for the Synoptic Scale Processes

LADCO compared modeled surface pressure, precipitation, and divergence winds with observation-based weather maps for high pollution episodic periods in 2022. Figure 3 shows time series of state–average daily maximum 8-hour average ozone (MDA8 O_3) and 24-hour average fine particulate matter ($PM_{2.5}$) concentrations in the Midwest for the year of 2022. Gray bars in the figure represent days influenced by fire smoke. These days are identified based on two conditions: (1) state-wide mean standard concentration anomaly greater than 1.5 and (2) HMS smoke presence in the column. Throughout 2022, there were several periods of elevated $PM_{2.5}$ and O_3 concentrations, including five notable episodes where both pollutants increased due to the transport of wildland fire smoke into the region. Among these, the period of June 14-22 had the highest peak for both pollutants. During this time, wildland fire smoke from Arizona, New Mexico, and Alaska, combined with smoke from prescribed fires in Iowa, Missouri, and Illinois, reached the LADCO region. This resulted in an initial rise in $PM_{2.5}$ concentrations, followed by an increase in MDA8 O_3 concentrations later in the period.

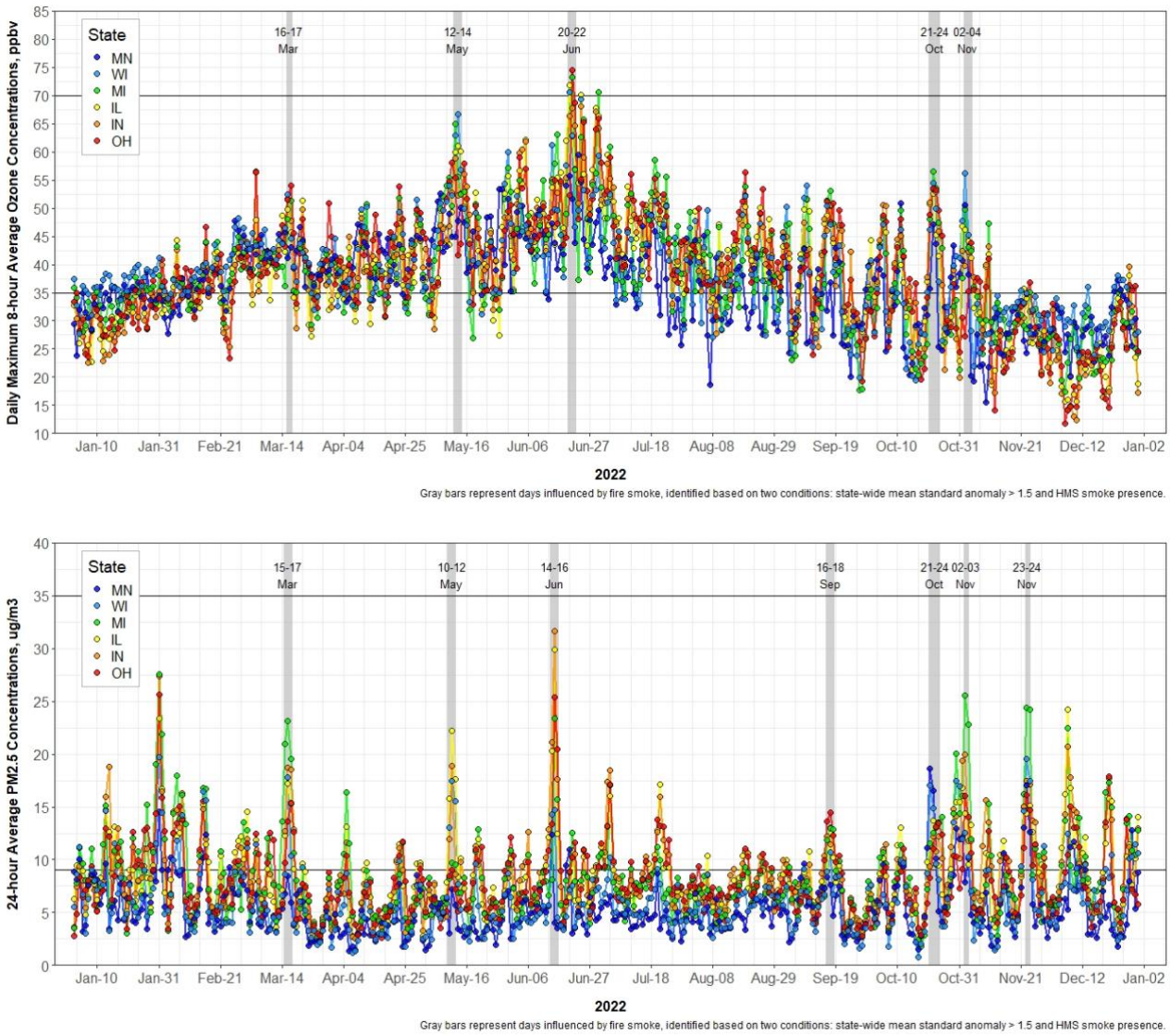

Figure 3. Daily maximum 8-hour average ozone concentrations (top) and 24-hour average fine particulate matter concentrations (bottom), averaged by all monitors within each state in the Midwest, 2022

Figure 4 and Figure 5 show comparisons of surface weather maps with 12-km resolution WRF model results for June 14-16 and June 20-22, respectively. As discussed above, we selected these dates for analysis because various areas in the region experienced elevated $PM_{2.5}$ and MDA8 O_3 surface concentrations during these periods. The National Centers for Environmental Prediction (NCEP), Hydrometeorological Prediction Center, National Weather Service[5] surface weather

[5] https://www.wpc.ncep.noaa.gov/dailywxmap/explaination.html

maps show the surface pressure isobars as solid lines in 4 mbar intervals and are annotated with centers of high- and low-pressure systems. Surface temperature isotherms are shown as dashed blue lines in 10^{o}C intervals. The maps show cold and warm fronts in blue or red, and areas with 6-hour accumulated precipitation in green. LADCO created model-based surface maps using the 12-km and 4-km WRF outputs of the surface pressure, precipitation, and divergence winds to indicate fronts and pressure system centers.

The comparisons of the NCEP and 12-km WRF surface maps in these figures show that WRF simulates well the extent and location of the high-pressure and low-pressure systems, cold fronts, trough lines, and precipitation in the contiguous U.S. For the $PM_{2.5}$ and O_3 episodes during June 2022 WRF captures well the locations and magnitudes of the high- and low-pressure systems in the Midwest at both 12-km and 4-km resolution, with surface pressure differences less than 2 hPa in the earlier morning (7:00 am EST).

.

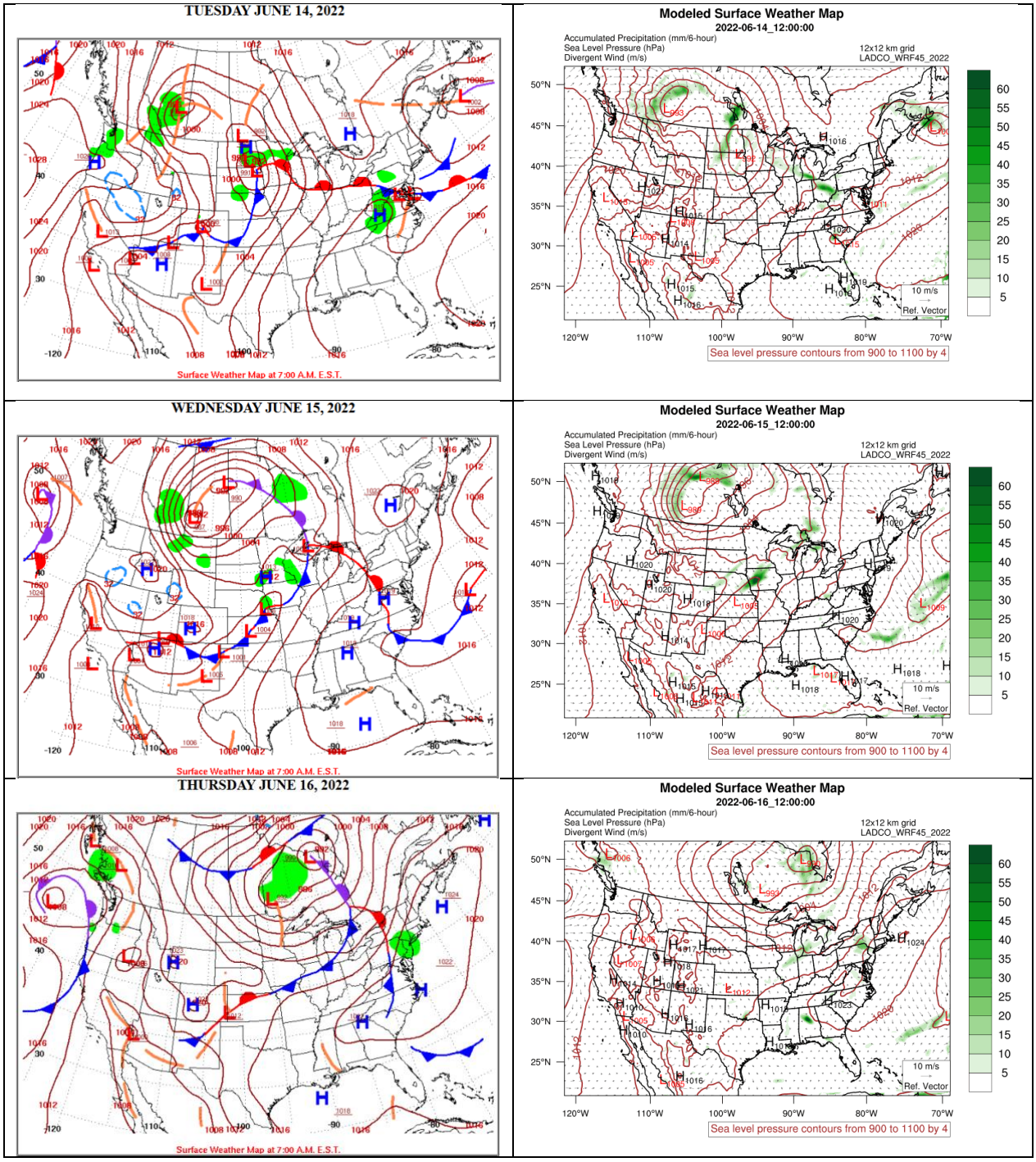

Figure 4. Comparison of surface weather maps with 12-km WRF modeled outputs at 12:00 pm UTC for June 14-16, 2022

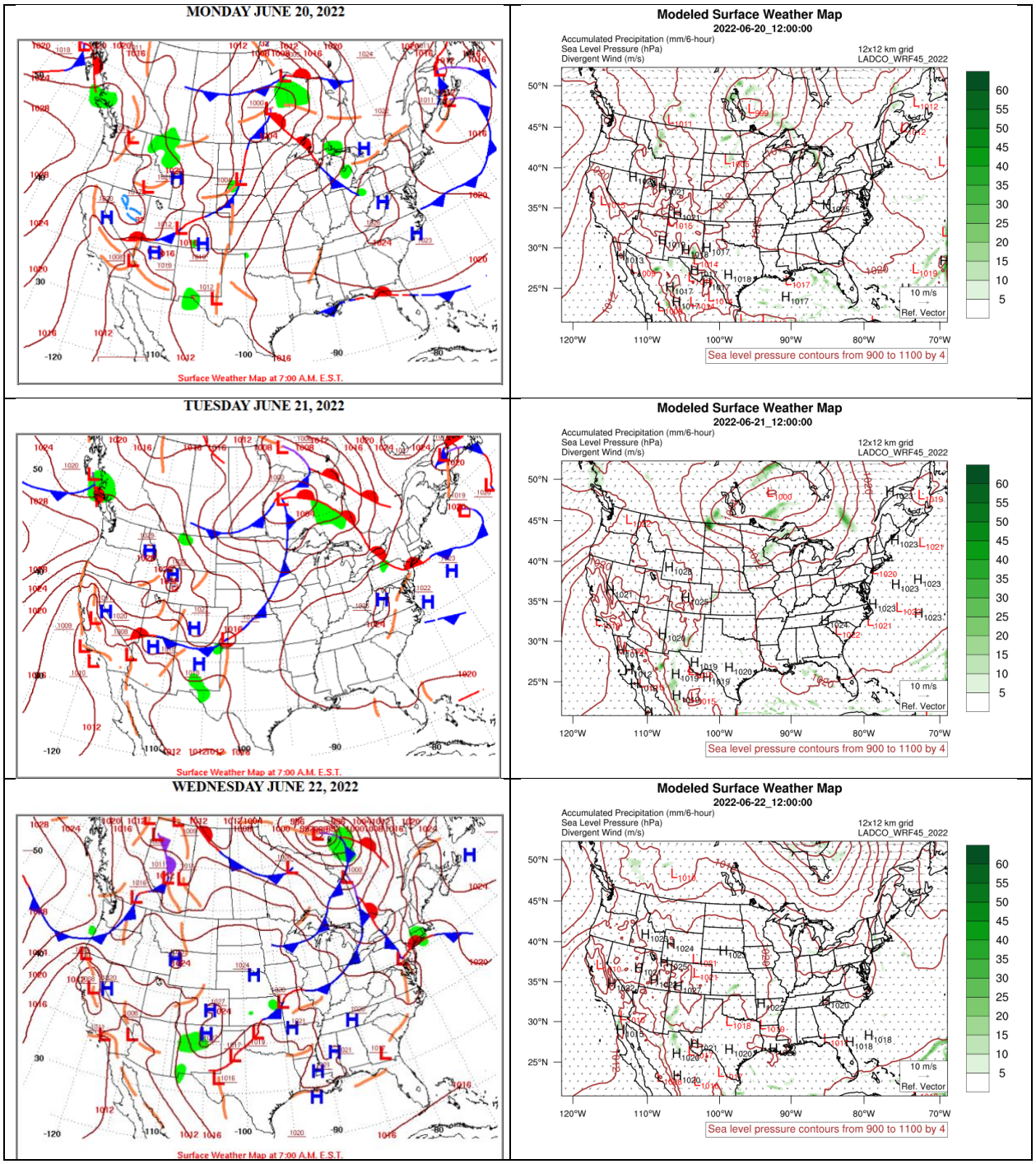

Figure 5. Comparison of surface weather maps with 12-km WRF modeled outputs at 12:00 pm UTC for June 20-22, 2022

Figure 6 and Figure 7 show that the 12-km and 4-km WRF simulations produced similar surface conditions as the NCEP analysis. Figure 6 shows good agreement between the surface maps and the WRF results for high- and low-pressure system locations associated with an active low-pressure system centered on western Minnesota on June 14, 2022, and the evolution of the system's cold and warm fronts in the Great Lakes region on the following two days. A warm front crossing over Lake Michigan from the northwest on June 14, 2022 is seen in both the 12-km and 4-km WRF simulations as a narrow precipitation band moving across the region. The WRF runs also produced the observed cold front on the eastern edge of the 4-km domain on Jun 15-16, 2022. Similarities in the locations of high- and low-pressure system centers, and in wind speeds and directions for the two different grid resolutions are due to a use of same NAM-HRRR data assimilation for both grids. Figure 6 also shows that that 4-km grid simulation was able to reproduce the features of an occluded cyclone (i.e., the dissipation of the low-pressure system) that formed over Lake Superior on June 15. In addition, the observed precipitation features such as location and intensity along the cold front, were simulated well on these days. Similarly, the model successfully simulated a low-pressure system formed over Manitoba, Canada, and its development during June 20-22, 2022 (Figure 7).

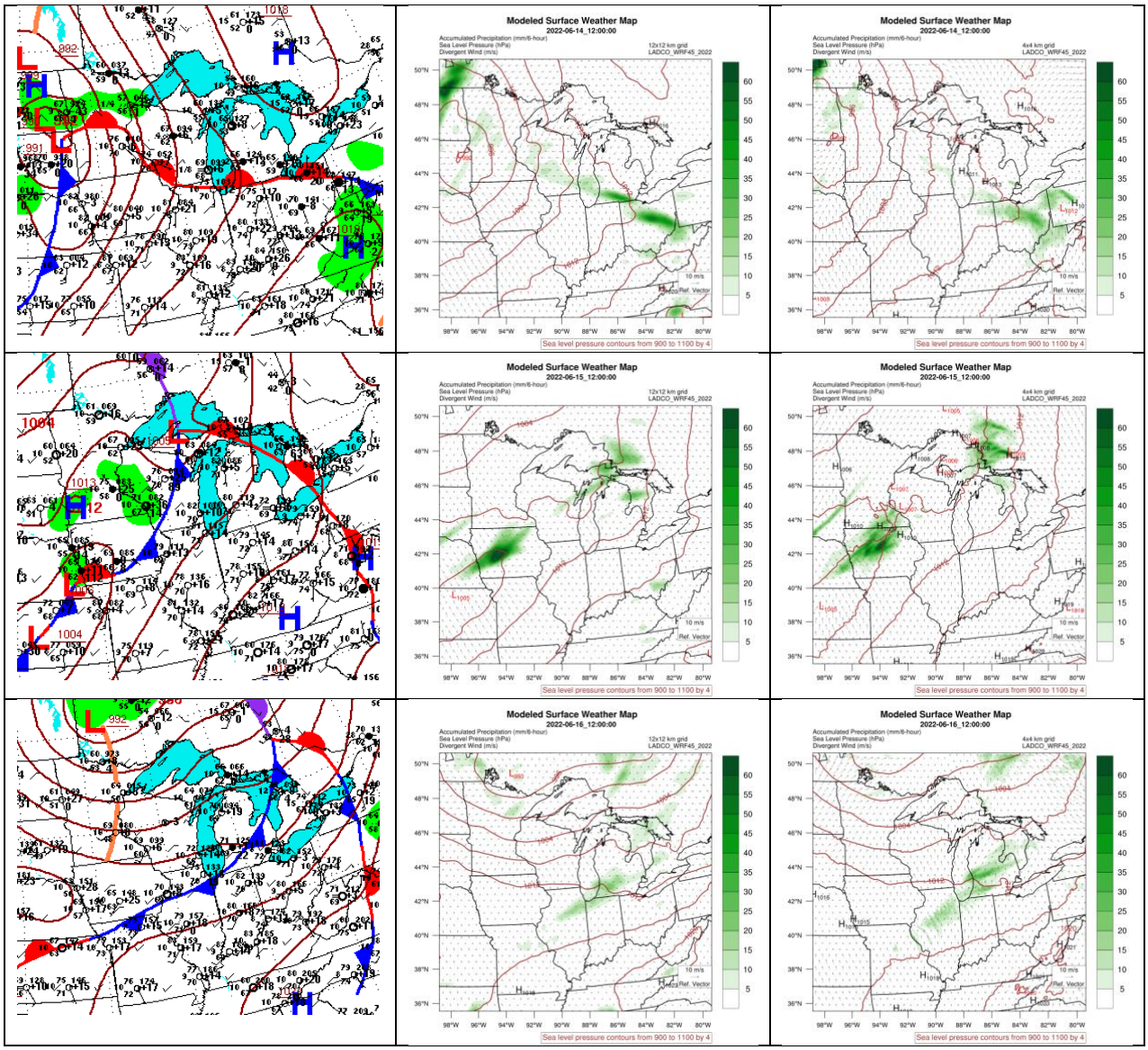

Figure 6. Comparison of surface weather maps with 12-km and 4-km WRF modeled outputs at 12:00 pm UTC for June 14-16, 2022

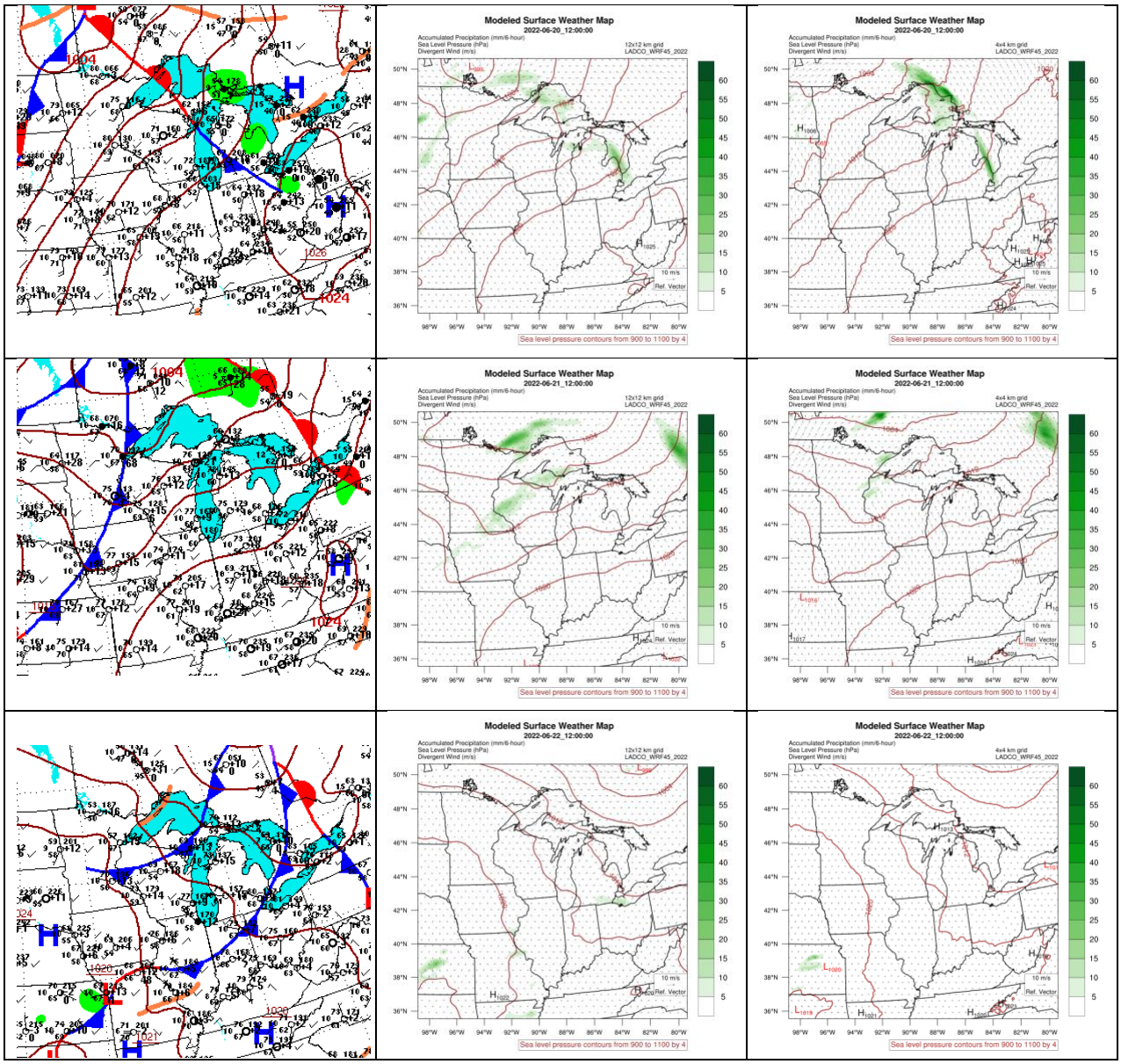

Figure 7. Comparison of surface weather maps with 12-km and 4-km WRF modeled outputs at 12:00 pm UTC for June 20-22, 2022

Overall, as shown in these surface map comparisons the 12-km and 4-km WRF simulations captured well the observed meso- and synoptic-scale processes during these periods. At these scales, the LADCO WRF 2022 output fields represent an acceptable approximation of the actual meteorology that occurred in 2022.

3.3 Region and State-level Model Performance Statistics

The following sections present the LADCO WRF 2022 model performance at surface METAR network monitors for temperature, specific humidity, wind speed, and wind direction. Average statistics are provided across the following dimensions for each of the WRF modeling domains:

- CONUS 12-km (d01): by season and monitors in each MJO
- LADCO 4-km (d02): by month and monitors in each state
- LADCO 1.33-km (d03): by month and monitors in the model domain

The average mean absolute errors (MAE) and mean biases (MB) of the key meteorology variables are derived by averaging all hourly performance statistics for a particular month or season across all METAR meteorological stations within the evaluation domain region.

3.3.1 CONUS12 WRF Model Performance

Table 5 summarizes the WRF 12-km domain-wide model performance by season. Spatial plots for the WRF model performance at surface sites in the CONUS12 domain for 2-meter temperature, 2-meter specific humidity, 10-meter wind speed, and 10-meter wind direction for each season are shown in Appendix A.1 These performance plots depict the seasonal model MB (colors) and MAE (circle size) at each monitor simulated by the WRF model. Figure 23 through Figure 26 show the seasonal MAEs and MBs of the 2-meter temperature predictions across the MJO regions. These figures show that overall, the temperature estimates are in exceptionally good agreement with observations. The estimated temperatures across the regions and seasons have about 1 K errors with near zero biases except for the West. The LADCO WRF modeling produced the largest errors in the Rocky Mountain and California valley areas (1.5±0.6 K MAEs) with a tendency of

cold biases in warmer seasons and warmer biases in cold seasons. Similar but less pronounced biases also occur in Texas and a few coastal locations around the Great Lakes.

Figure 27 through Figure 30 summarize the 12-km WRF 2-meter specific humidity (i.e., water vapor mixing ratio) performance. The LADCO 2022 12-km WRF simulation has very slight positive biases (0.1-0.5 g/kg MBs) and low errors (0.2-1.7 g/kg MAEs) depending on region and season. The magnitude and regional variability of MAEs for specific humidity are lower in winter (0.4±0.2 k/kg) compared to the summer (1.4±0.4 k/kg). Specific humidity is unbiased in winter across the domain, but is slightly overestimated in summer and fall, with mean biases of 0.4 k/kg in the LADCO region, about 0.6 g/kg in the West and South Central. The model underestimated humidity in the Gulf Coast and Florida by about -0.6 g/kg. The model fails to simulate the enhanced water vapor mixing ratio due to convective activity in the South Central, and the influx of moist air masses from the Gulf Mexico and Southeast coast, and riparian area of the Mississippi River in summer. In general, the 12-km WRF performance for water vapor mixing ratio was acceptable and within the commonly used benchmark, except for the Southwest, Texas, Florida, and Gulf coast in the summer.

Figure 31 through Figure 34 summarize the 10-meter wind speed performance of the LADCO 2022 12-km WRF simulation. The modeled surface wind speeds are in good agreement with observations throughout the domain and season. Regional average errors (1.1±0.4 m/s) and biases (-0.3±0.7 m/s) are within the benchmark criteria of 2.0 m/s MAE and ±0.5 m/s MB for typical meteorological conditions. Overall, the LADCO 2022 12-km WRF simulation of wind speed tends to underestimate across the MJO regions and seasons, especially in the West and South with moderate negative biases (- 0.6 m/s) for all season around. Wind speed estimates tend to have lesser errors and near-zero biases in the East and the Midwest.

Figure 35 through Figure 38 summarize the 10-meter wind direction performance of the LADCO 2022 12-km WRF simulation. The WRF wind direction predictions exhibit the lowest MAEs in the LADCO region (23-35°) across all seasons, while MAEs are higher in all other regions (31-58°), with error levels varying by region depending on the season. The highest MAEs (56-58°) seen in the West, South, Southeast, and Appalachian Mountains that persist throughout the year along with more prominent in spring and summer could be explained by the fact the wind direction

errors increase with underestimation of the wind speed (-0.7 m/s MB), which is triggered by the model overestimation of specific humidity (0.5 g/kg MB) in the warm seasons. This indicates that the model did not accurately resolve the orographic effects and summertime convective processes in these complex terrain regions. In addition, wind direction estimates in the Gulf of Mexico and Southeast coastal states were adversely impacted by the Category 4 hurricanes Fiona and Ian that occurred in September 2022. Nonetheless, the model estimates for the wind direction met the benchmark for the complex meteorological condition for these regions. The 12-km WRF wind direction predictions are the best for the LADCO region as compared to other MJO regions. The mean MAE is about 24 degrees in cold seasons and about 30 degrees in warm seasons for the LADCO region.

It is not easy to interpret wind direction biases in the larger temporal scale such as monthly or seasonally without a knowledge of observed wind direction at stations. In general, positive (negative) biases in the wind direction indicate that modeled wind direction is shifted clockwise (counterclockwise) relative to the observed wind direction at a monitoring station. Considering that complex mesoscale weather systems occurred during 2022 (National climate Report, 2022 National Overview[6]), the LADCO 2022 12-km WRF wind direction estimates are considered reasonable when compared to the complex terrain model performance benchmark of 55 degrees (Kemball-Cook et al., 2005).

Overall, the LADCO 2022 WRF simulation of surface meteorological variables is in good agreement with observations. The WRF performance statistics for the 12-km grid resolution simulation are within the acceptable performance benchmarks proposed by Emery et al. (2001) and Kemball-Cook et al. (2005) for air quality model applications. In summary, the LADCO 2022 12-km WRF simulated temperatures very well across the domain, and slightly overestimated specific humidity, especially in the West and South Central in summer. The model tends to underestimate wind speed across all seasons, which led to larger errors in wind direction in the West, South Central and Southeast coastal states in all seasons except for spring.

[6] Annual 2022 National climate Report - National Overview

.

Table 5. 2022 seasonal average 12-km WRF model performance for entire 12US2 domain

Season*	Temp2m (K)		MixingRatio2m (g/kg)		WS10m (m/s)		WD10m (degrees)	
	MAE	MB	MAE	MB	MAE	MB	MAE	MB
Winter (DJF)	1.2	0.0	0.5	0.2	1.1	-0.2	39.2	2.8
Spring (MAM)	1.2	-0.1	0.8	0.3	1.2	-0.4	36.5	3.7
Summer (JJA)	1.2	-0.1	1.5	0.3	1.1	-0.5	42.8	2.4
Fall (SON)	1.2	0.0	0.9	0.3	1.1	-0.3	42.4	1.7

*Green shading indicates a metric that meets the performance benchmarks for simple conditions, orange for complex conditions, and red for outside of the performance benchmarks

3.3.2 WRF 12-km Performance Summary for the LADCO region

Table 6 summarizes the seasonal LADCO 2022 12-km WRF model performance for the part of the domain covering only the LADCO states. The LADCO 12-km WRF run for the LADCO region has average MAEs of 1.1 K for temperature, about 0.7 g/kg for specific humidify, about 1 m/s for wind speed and 28 degrees for wind speed. On average, the 12-km model run predicted a slightly cooler and wetter winter, and slightly wetter summer in the LADCO region relative to the observations, although performance statistics are all well below the model performance benchmarks.

Table 6. 2022 seasonal average 12-km WRF model performance for the LADCO states

Season*	Temp2m (K)		MixingRatio2m (g/kg)		WS10m (m/s)		WD10m (degrees)	
	MAE	MB	MAE	MB	MAE	MB	MAE	MB
Winter (DJF)	1.0	-0.2	0.2	0.1	1.0	0.0	22.8	3.3
Spring (MAM)	1.1	-0.2	0.6	0.3	1.1	-0.2	26.4	1.0
Summer (JJA)	1.1	0.0	1.2	0.4	1.0	-0.2	34.8	1.2
Fall (SON)	1.1	-0.1	0.6	0.3	0.0	0.2	26.2	2.4

*Green shading indicates a metric that meets the performance benchmarks for simple conditions, orange for complex conditions, and red for outside of the performance benchmarks

3.3.3 Model Performance for the 4-km LADCO Domain

Table 7 summarizes the domain-wide model performance of the LADCO 2022 4-km WRF simulation for the key surface meteorological variable by season. The spatial plot of the summer (June-August) model performance for temperature, specific humidity, wind speed, and wind

direction are shown in Figure 8 through Figure 11 along with aggregated statistics by state. The winter and summer model performance at 4-km resolution for the LADCO states are summarized in Table 8 and 9, respectively.

In general, the state-specific performance for the LADCO 2022 4-km WRF simulation for summer season surface temperature, specific humidity, and wind speed was better (MAE = 1.1-1.2 K; MAE = 0.3-1.2 g/kg; MAE = 1.0-1.1 m/s) than the performance statistics that were averaged across the entire modeling domain. The model has slight positive biases in both temperature and specific humidity (i.e., model estimated slightly warmer and wetter air than observed with MB = 0.2±0.4 K and 0.5±0.5 g/kg, respectively) across the LADCO states in the summer. The LADCO 2022 4-km WRF simulation has similar performance statistics as those for 12-km simulation (Table 6).

Table 7. 2022 seasonal average 4-km WRF model performance for entire LADCO4 domain

Season*	Temp2m (K)		MixingRatio2m (g/kg)		WS10m (m/s)		WD10m (degrees)	
	MAE	MB	MAE	MB	MAE	MB	MAE	MB
Winter (DJF)	1.1	0.0	0.3	0.2	1.1	-0.1	27.9	3.6
Spring (MAM)	1.1	0.0	0.7	0.3	1.1	-0.2	28.8	1.5
Summer (JJA)	1.1	0.2	1.2	0.4	1.0	-0.1	37.7	1.2
Fall (SON)	1.2	0.0	0.7	0.3	1.0	0.1	30.9	1.5

*Green shading indicates a metric that meets the performance benchmarks for simple conditions, orange for complex conditions, and red for outside of the performance benchmarks

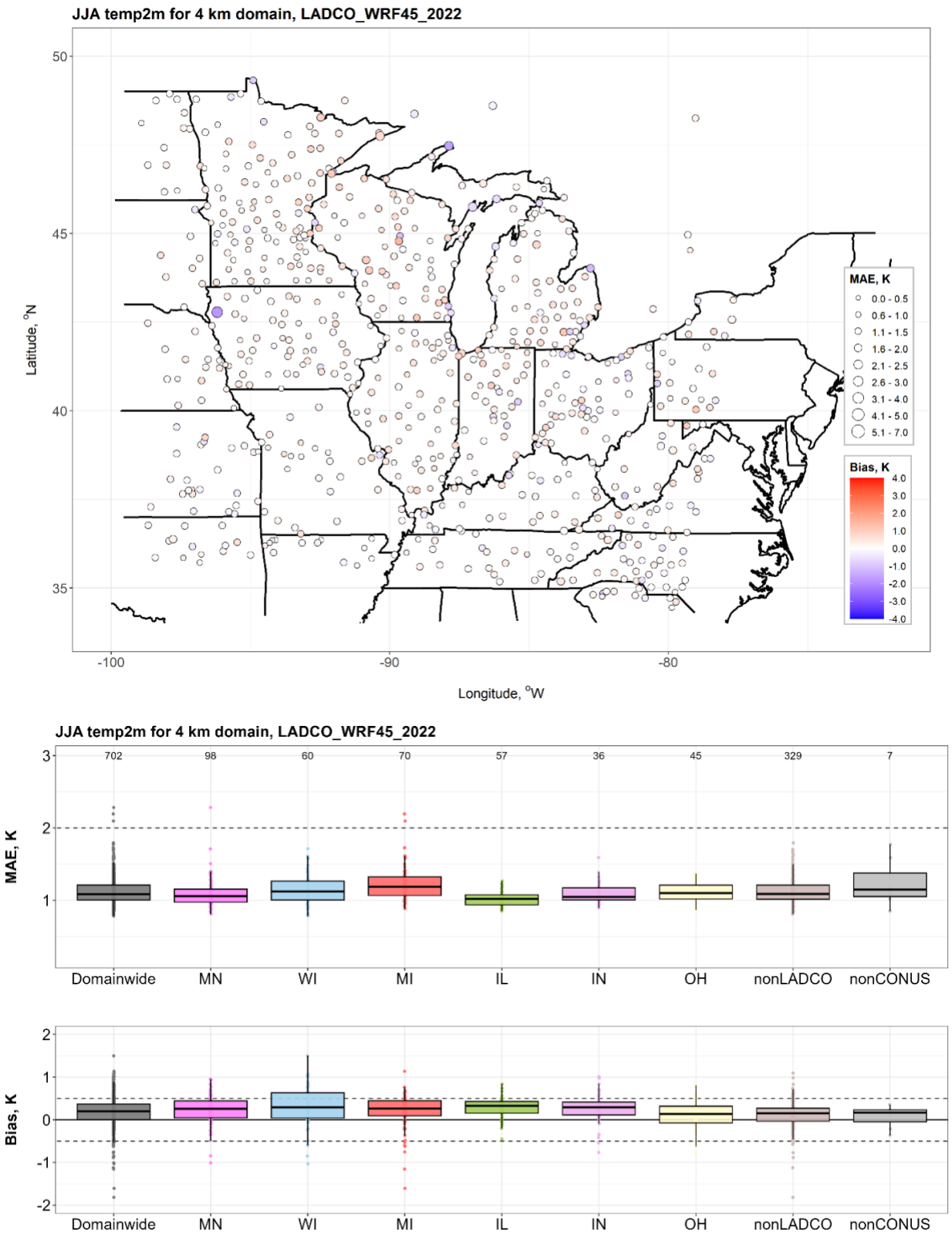

Figure 8. Mean Absolute Errors and Biases for Temperature in the 4km Domain, Summer 2022

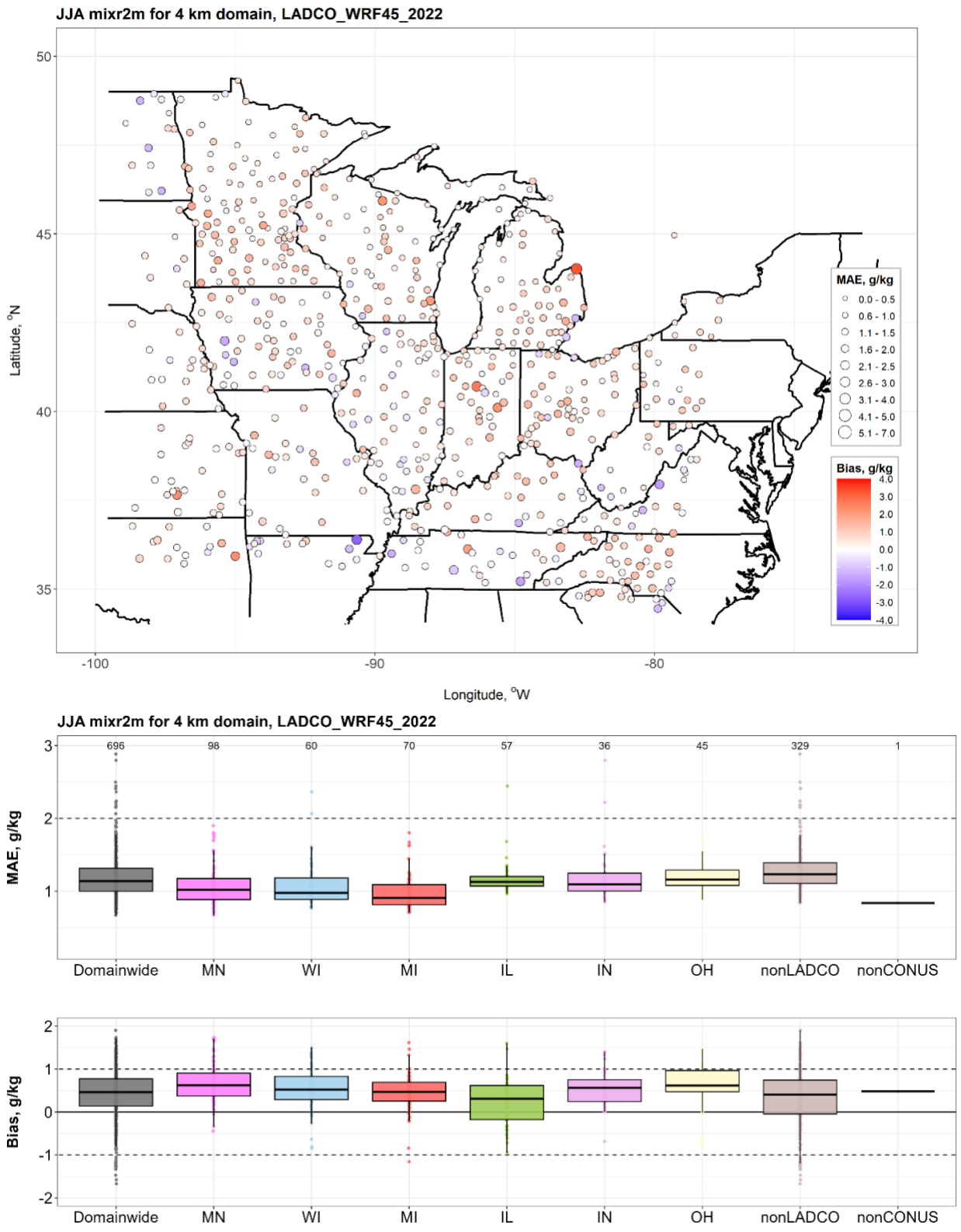

Figure 9. Mean absolute errors and biases for specific humidity in the 4km domain, Summer 2022

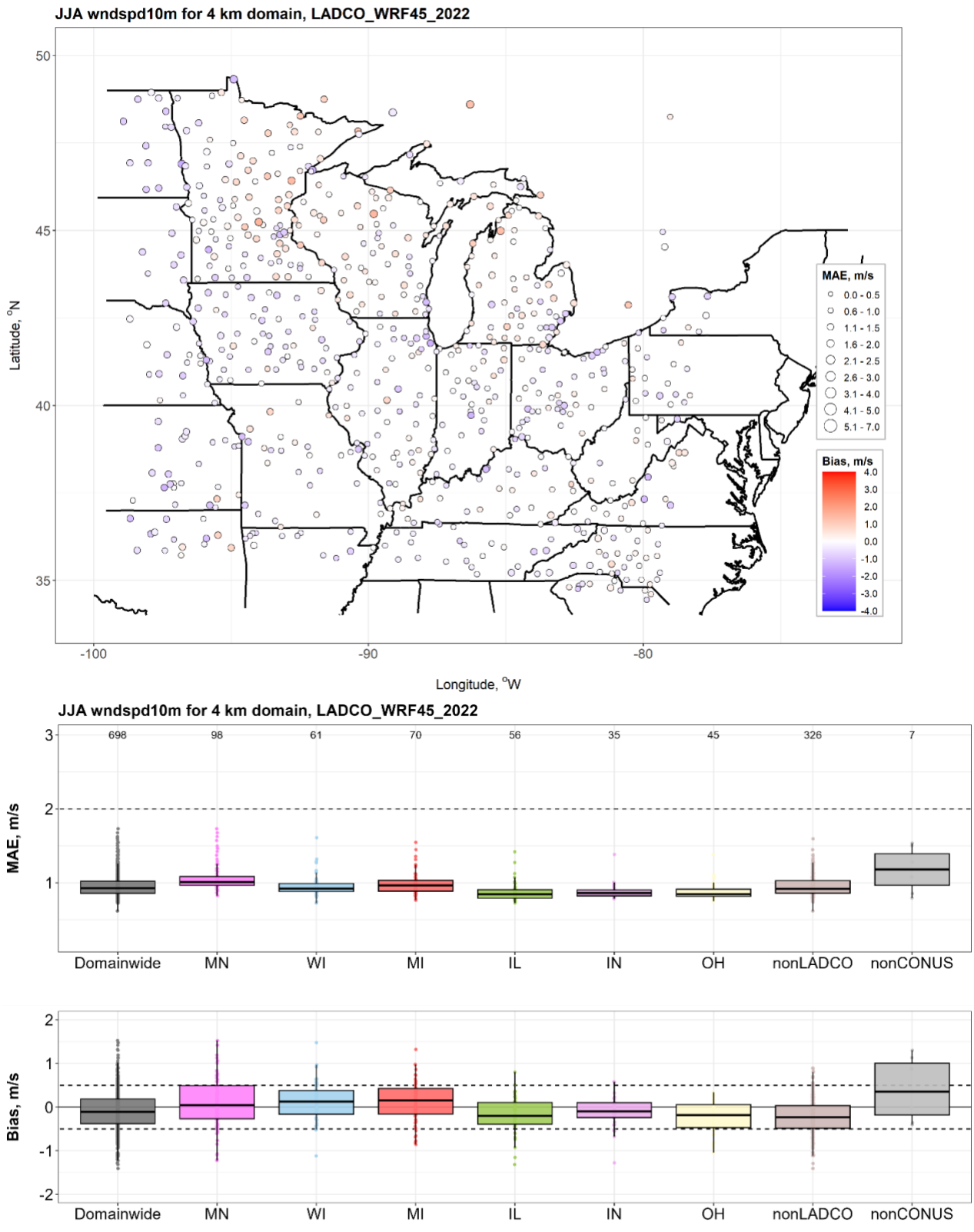

Figure 10. Mean absolute errors and biases for wind speed in the 4km domain, Summer 2022

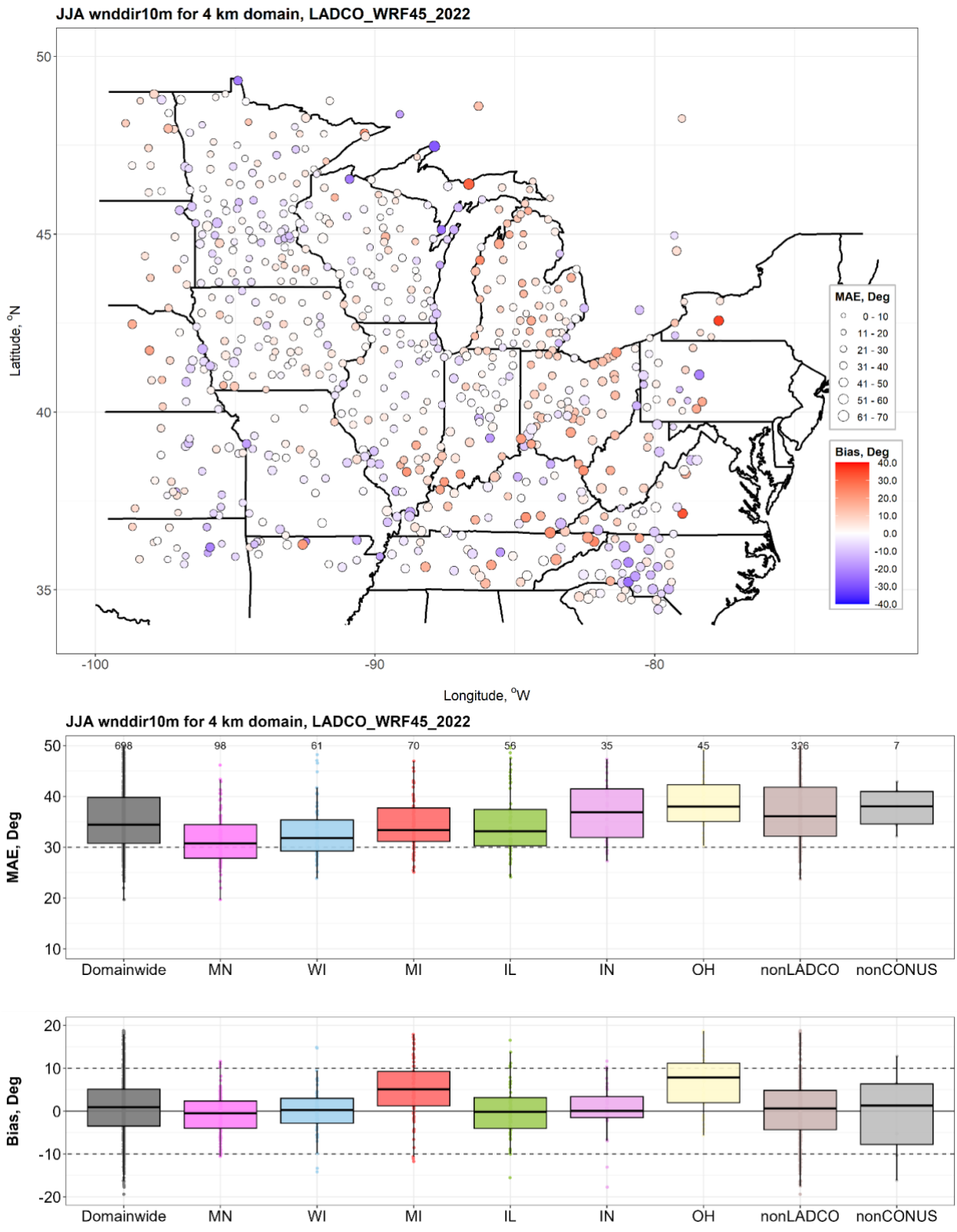

Figure 11. Mean absolute errors and biases for wind direction in the 4km domain, Summer 2022

.

3.3.4 WRF 4-km Performance Summary for the LADCO states

Table 8 and Table 9 summarize the summer and winter model performances aggregated by all monitors located in each of the LADCO states. All summer and winter metrics, except wind direction error, are well below the simple terrain model performance benchmarks, while the summer wind direction error falls within the complex terrain benchmark. On average, the temperature and wind speed errors are about 1K or 1m/s for both the winter and summer season, the specific humidity and wind direction errors are much smaller in the winter than those in the summer.

Table 8. 2022 summer season (JJA) 4-km WRF model performance for the LADCO states

State*	Temp2m (K)		MixingRatio2m (g/kg)		WS10m (m/s)		WD10m (degrees)	
	MAE	MB	MAE	MB	MAE	MB	MAE	MB
IL	1.0	0.3	1.2	0.2	0.9	-0.2	35.8	0.0
IN	1.1	0.3	1.2	0.6	0.9	-0.1	37.1	1.6
MI	1.2	0.2	1.0	0.5	1.0	0.1	35.6	4.7
MN	1.1	0.2	1.1	0.7	1.1	0.1	31.9	-0.8
OH	1.1	0.1	1.2	0.6	0.9	-0.2	41.0	7.1
WI	1.1	0.3	1.1	0.6	1.0	0.1	33.3	-0.2

*Green shading indicates a metric that meets the performance benchmarks for simple conditions, orange for complex conditions, and red for outside of the performance benchmarks

Table 9. 2022 winter season (DJF) 4-km WRF model performance for the LADCO states

State*	Temp2m (K)		MixingRatio2m (g/kg)		WS10m (m/s)		WD10m (degrees)	
	MAE	MB	MAE	MB	MAE	MB	MAE	MB
IL	0.9	0.0	0.3	0.1	1.1	-0.3	24.5	3.6
IN	0.9	0.0	0.3	0.2	1.0	0.0	21.4	3.9
MI	1.0	0.0	0.2	0.1	1.1	0.2	26.7	4.4
MN	1.2	0.0	0.2	0.1	1.1	0.0	22.5	4.6
OH	1.0	-0.2	0.4	0.3	1.0	-0.2	25.3	6.6
WI	1.2	0.2	0.2	0.1	1.1	0.3	22.5	6.0

*Green shading indicates a metric that meets the performance benchmarks for simple conditions, orange for complex conditions, and red for outside of the performance benchmarks

3.3.5 Model Performance for the 1.33 km domains

LADCO used WRF to simulate meteorology over a 1.33-km domain covering Lake Michigan and surrounding areas for April through September 2022. Figure 12 shows summertime MAE and MB for surface temperature, water vapor, wind speed and wind direction. Table 10 shows that overall, the LADCO 2022 1.33 km WRF simulations are exceptional. The model performance statistics averaged over all stations with the 1.3-km domain are well within the model performance benchmarks.

The seasonal average statistics are based on 90-100 surface meteorological stations depending on variable and domain. The 2-m temperature MAE was 1.3±0.6°K, the 2-m specific humidity MAE was 1.0±0.8 g/kg, the 10-m wind speed MAE was 1.2±0.7 m/s, and the 10-m wind direction was 34.8°±8.3. The model estimates are mostly unbiased at stations, except for slight overestimation at few stations in both domains.

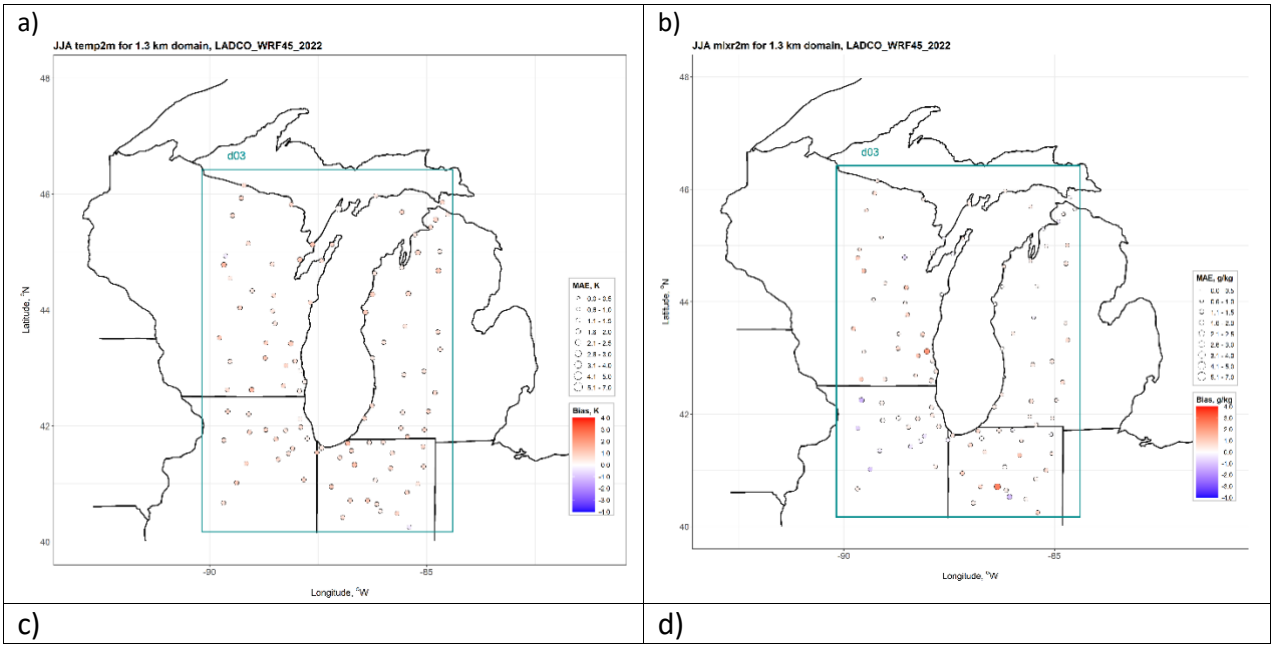

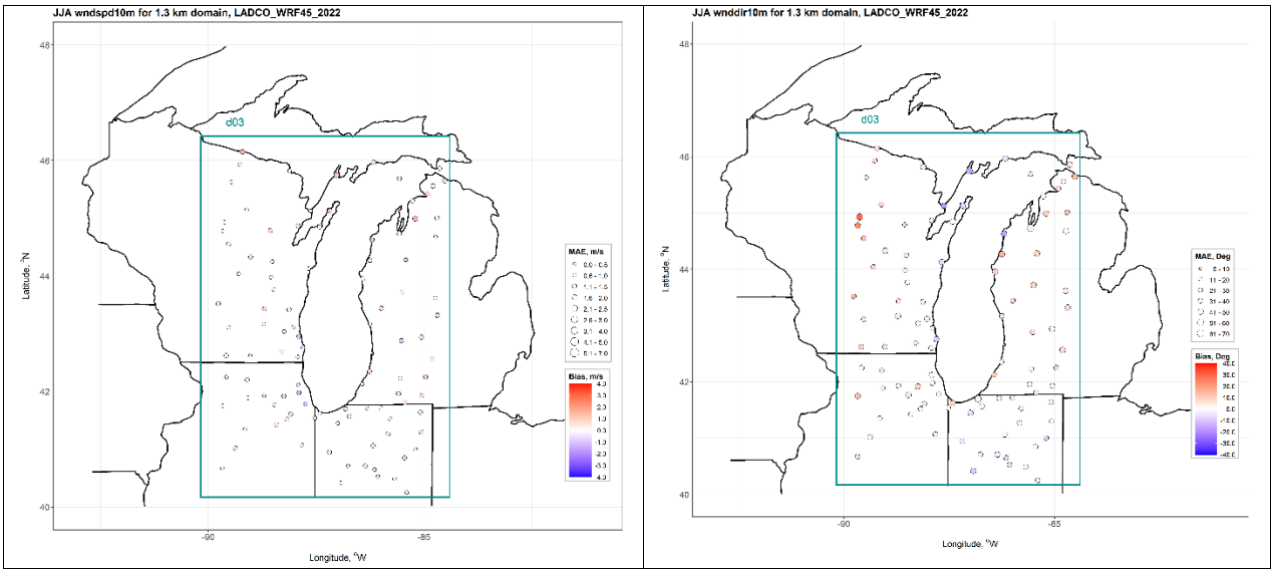

Figure 12. Mean absolute errors and biases for air temperature (a), specific humidity (b), wind speed (c) and wind direction (d) in the 1.33km domains, summer (JJA) 2022

Table 10. 2022 seasonal average model performance statistics for the 1.33-km Lake Michigan domain

Season*	Temp2m (K)		MixingRatio2m (g/kg)		WS10m (m/s)		WD10m (degrees)	
	MAE	MB	MAE	MB	MAE	MB	MAE	MB
Spring (AM)	1.4	0.2	0.7	0.3	1.2	0.0	28.5	2.9
Summer (JJA)	1.4	0.7	1.1	0.3	1.1	0.2	38.6	2.7
Fall (SO)	1.3	0.5	0.8	0.1	1.0	0.3	37.6	1.9

*Green shading indicates a metric that meets the performance benchmarks for simple conditions, orange for complex conditions, and red for outside of the performance benchmarks

3.3.6 LADCO 2022 WRF Spatial Scale Performance Summary

We calculated the LADCO WRF 2022 summer season model performance at a common set of surface stations across grid resolutions to see how model performance varies by the grid resolution. There are about 103 METAR stations located in the 1.33 km domain. Table 11 tabulates summer season (JJA) WRF performance at 12-km, 4-km, and 1.3-km grid resolutions. Model errors for temperature, humidity, and wind director decreased by about 10% in the 4-km simulation relative to the 12-km simulation. The model errors increased for all variables in the 1.3-km simulation relative to the 4-km simulation Although the 1.3-km simulation did not

produce a significant summer season performance improvement, the model resolved well local-scale convective processes and had a better performance (specifically, lesser wind direction errors) during the lake-breeze afternoon hours, which are discussed in Section 5.

Table 11. 2022 summer season (JJA) WRF model performance for common locations in the three LADCO WRF modeling domains

Domain	Temp2m (K)		MixingRatio2m (g/kg)		WS10m (m/s)		WD10m (degrees)	
	MAE	MB	MAE	MB	MAE	MB	MAE	MB
CONUS 12	1.2	0.0	1.1	0.3	0.9	-0.2	33.6	1.4
LADCO 4	1.1	0.2	1.0	0.5	0.9	0.0	33.4	1.7
LADCO 1.33	1.4	0.7	1.1	0.3	1.1	0.2	38.6	2.7

4 WRF Performance Evaluation for Lake-breeze Events

Elevated concentrations of surface ozone in the Great Lakes Basin are observed near the shorelines of the lakes. The dynamical features at the land-water interface are well-known to be conducive to ground-level ozone formation. The lake-breeze is a key meteorological phenomenon associated with high ozone conditions in the region. This section assesses the LADCO WRF 2022 simulation skill during representative lake-breeze events in 2022 that had led to the observed high ozone concentrations.

LADCO used qualitative and quantitative methods to evaluate how well the WRF model simulates lake-breeze events that occur on the shorelines of Lake Michigan. The qualitative evaluation includes comparisons of satellite imagery and observed wind fields with modeled PBL height and wind vectors. Statistical model performance at eleven METAR stations located near the shoreline are used for quantitative evaluation for lake-breeze events. The station locations are shown in Figure 13.

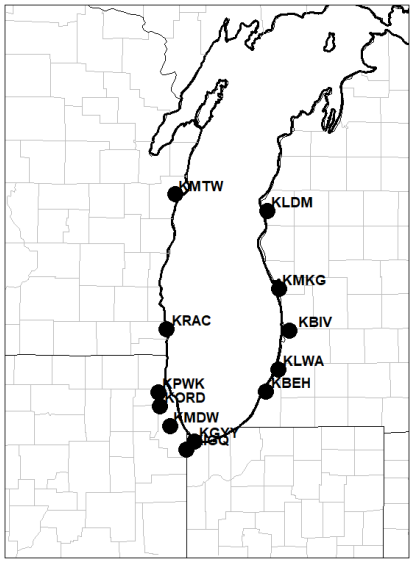

Figure 13. METAR stations on the shoreline of Lake Michigan. The stations are elevated less than 200 m a.s.l and located south of the 44°N latitude

We used time series and CART (Classification and Regression Tree)[7] analyses to identify the conditions at the surface meteorological stations that are associated with the identified lake-breeze days. The statistical software R version 4.2.3 and the R package rpart[8] was used for regressing the lake-breeze days explained by the hourly meteorological condition. We pruned the CART analysis trees using site-specific complexity parameters to increase the overall accuracy of the model and to minimize cross-validation errors. We then calculated and compared WRF performance statistics, such as mean absolute error and mean bias, using observed and WRF modeled values for the lake-breeze and non-lake-breeze days predicted by CART model for selected shoreline monitors.

4.1 Identifying Lake-breeze Days

LADCO analyzed daily cloud cover imagery, radar reflectance data, modeled wind fields from the Visible Infrared Imaging Radiometer Suite (VIIRS) Corrected Reflectance, the National Doppler Radar, and GFS reanalysis data for the period of April 1 to September 30, 2022, to identify lake-

[7] L. Breiman, J.H. Friedman, R.A. Olshen, and C.J Stone. Classification and Regression Trees. Wadsworth, Belmont, CA, 1983

[8] https://cran.r-project.org/web/packages/rpart/vignettes/longintro.pdf

breeze days along the Lake Michigan shore. Cloud cover imagery from the VIIRS instrument, which is on the joint NASA/NOAA Suomi National Polar orbiting Partnership (Suomi NPP) NOAA-20 polar orbiting satellite, is available through NASA Worldview and the Global Imagery Browse Services (GIBS, https://worldview.earthdata.nasa.gov/). High-definition reflectivity composite data prepared by the Environmental and Climate Change (1-km Radar Canada Section C) reveals visible features such as lake-breeze fronts or outflow boundaries and associated precipitation features near the land-water interface (https://weather.us/radar-us). Table 15 in Appendix A.2 shows the screening results of identified breeze days around Lake Michigan in summer 2022.

Both the VIIRS surface reflectance and radar imagery show fair weather low-to-mid level cumulus cloud fronts that penetrate inland during a lake-breeze event. These fronts are associated with rising, warm air masses over land that get replaced by relatively cold air masses originating over the lake during the summer season. The lake-breeze can be observed by local changes in lake-to-land winds, wind convergence over land, and wind divergence over the lake. The changes in winds can be indicated by numerical weather modeling results from the GFS/NCEP/ US National Weather Service (https://earth.nullschool.net).

Both the VIIRS and radar imagery indicated surface wind convergence zones due to a lake-breeze occurred for 34 days[9] in summer of 2022 along the shore of Lake Michigan.

As an example, the VIIRS surface reflectance, radar imagery and GFS modeled surface wind field in afternoon of June 29 and July 14, 2022, are shown in Figure 14 and Figure 15. The satellite and radar imagery show a lake-breeze front around Lake Michigan and surface wind divergence over the lake, which are typical features of lake-breeze events.

[9] Identified prior lake-breeze days around Lake Michigan shore: 4/3, 5/4, 5/23, 6/14, 6/23, 6/27, 6/29, 7/3, 7/5, 7/6, 7/7, 7/13, 7/14, 7/25, 7/26, 7/30, 7/31, 8/5, 8/9, 8/11, 8/16, 8/17, 8/18, 8/21, 8/22, 8/23, 8/24, 8/26, 9/3, 9/6, 9/7, 9/8, 9/10, 9/14

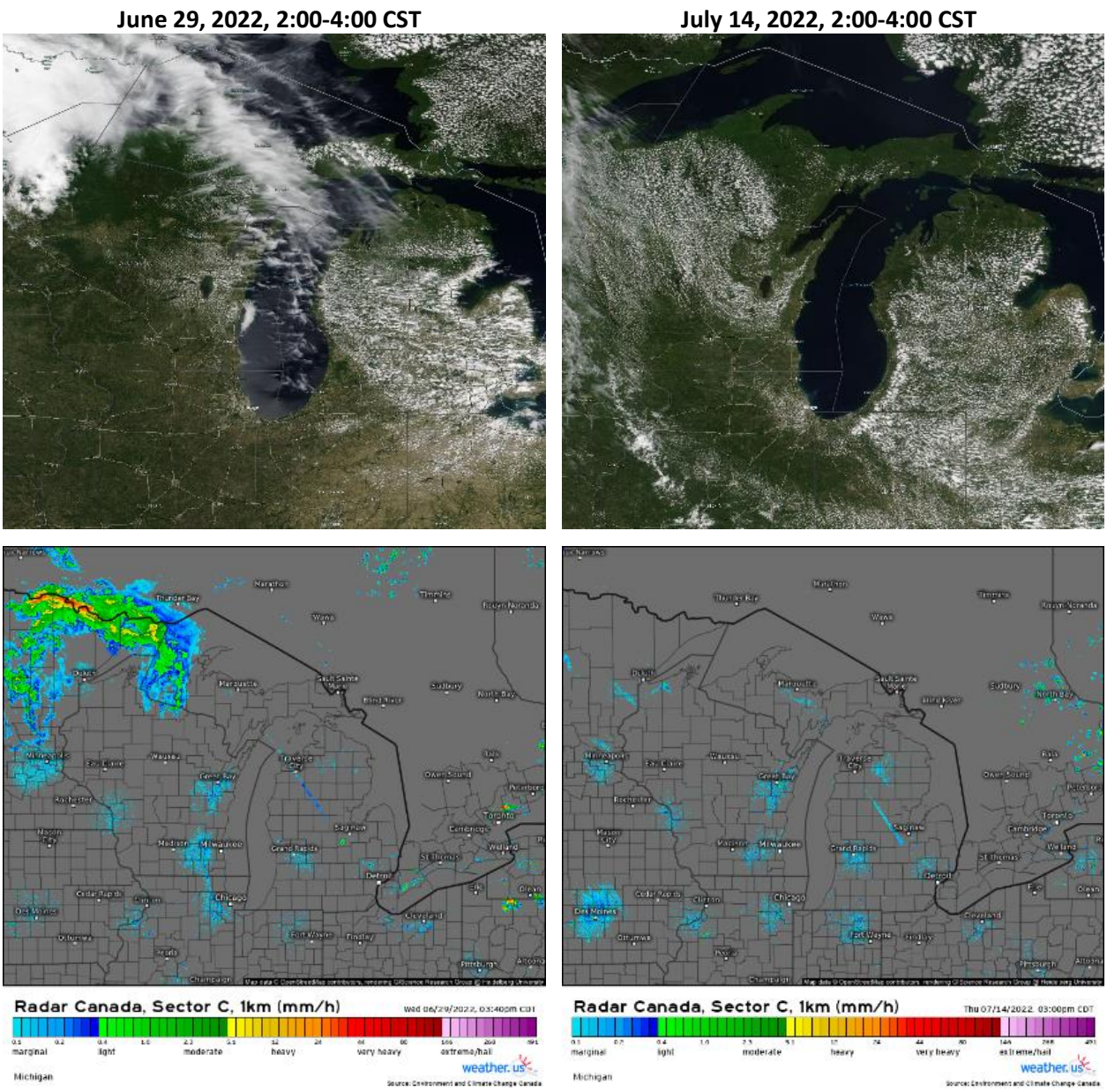

Figure 14. Lake-breeze front viewed by VIIRS satellite true color imagery (top) and radar reflective imagery (bottom) for June 29 (left) and July 14 (right), 2022

.

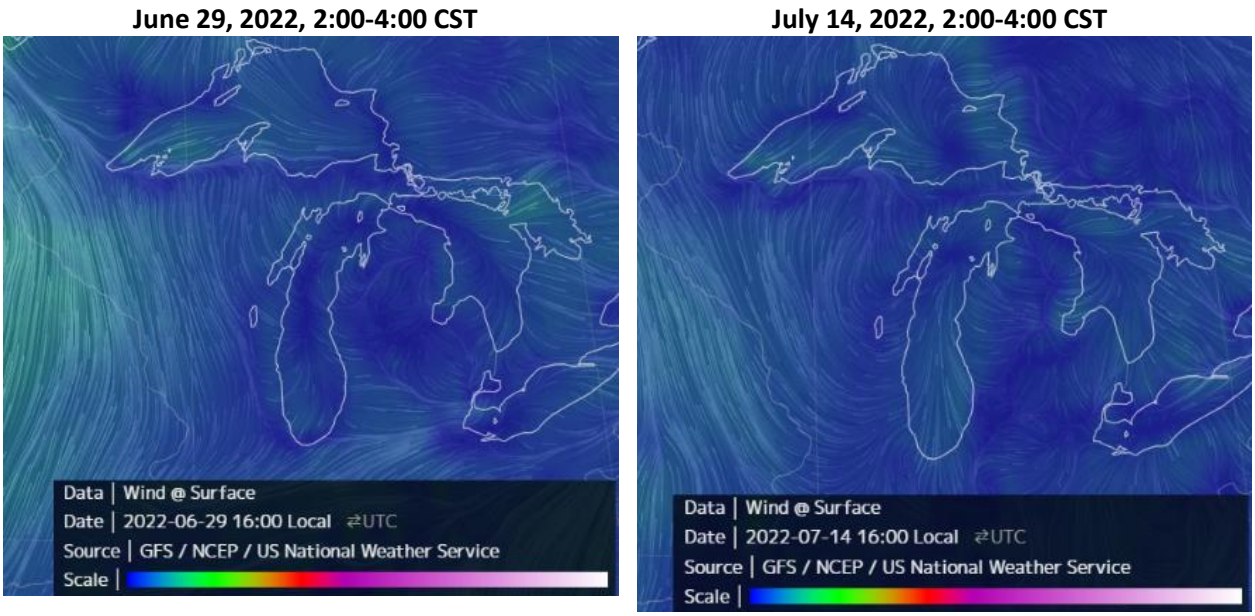

Figure 15. GFS model wind field in the Great Lakes for June 29 (left) and July 14 (right), 2022

To verify that the LADCO 2022 WRF modeling reproduced the features of the lake-breeze, we looked at simulated images of the predicted surface (10-m) winds, surface (2-m) temperatures, and planetary boundary layer (PBL) heights during the morning and afternoon hours on these days. In addition, we used classification and regression tree analysis (CART) to help us identify the meteorological conditions associated with identified lake-breeze days. Descriptions of the lake-breeze analysis and results follow.

4.2 Satellite Imagery Analysis

Figure 16 through Figure 18 depict lake-breeze fronts that formed around Lake Michigan on June 29, July 03, and July 14, 2022, respectively. The lake-breeze fronts are seen in the satellite true color imagery, and in the WRF modeled planetary boundary layer (PBL) height and wind fields. WRF simulated light to moderate north or north-easterly winds in the morning hours (before 09:00 CDT) over Lake Michigan on these days. The simulated winds shifted in the afternoon with divergence over the lake. WRF simulated a lake-to-land breeze with onshore convergence starting in the early afternoon that dissipated around 21:00 CDT on each day.

One notable feature of the WRF simulations is the weakening of the lake breeze intensity as the simulation grid resolution increased. In all three of the lake breeze events shown here, the inland convergence zones resolved closer to the lake shore at the finer grid resolutions. We speculate that the lack of FDDA in the 1.3 km domain penalized the model skill in resolving the extent of the lake breeze on these days.

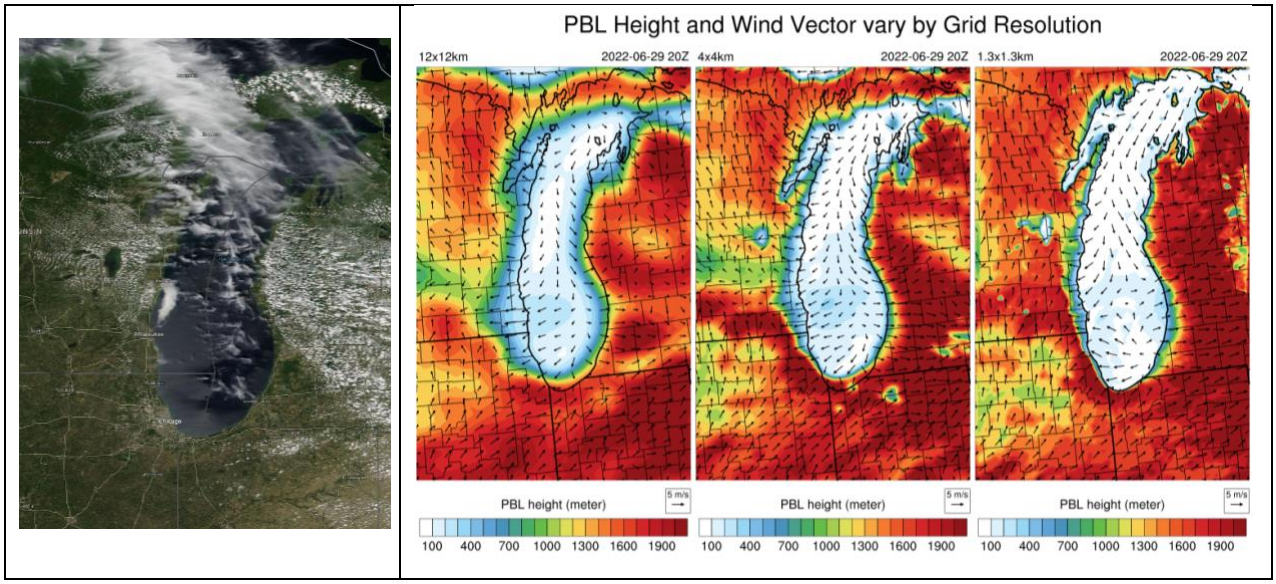

Figure 16. June 29, 2022 (14:00 CST) satellite imagery and modeled PBL height and wind vectors

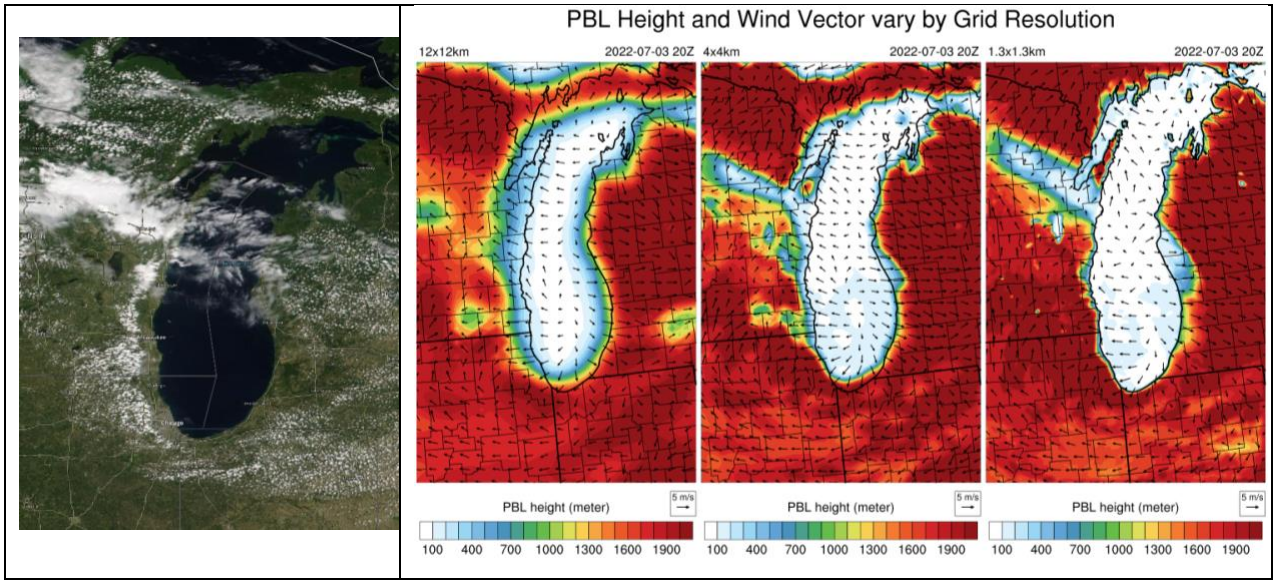

Figure 17. July 03, 2022 (14:00 CST) satellite imagery and modeled PBL height and wind vectors

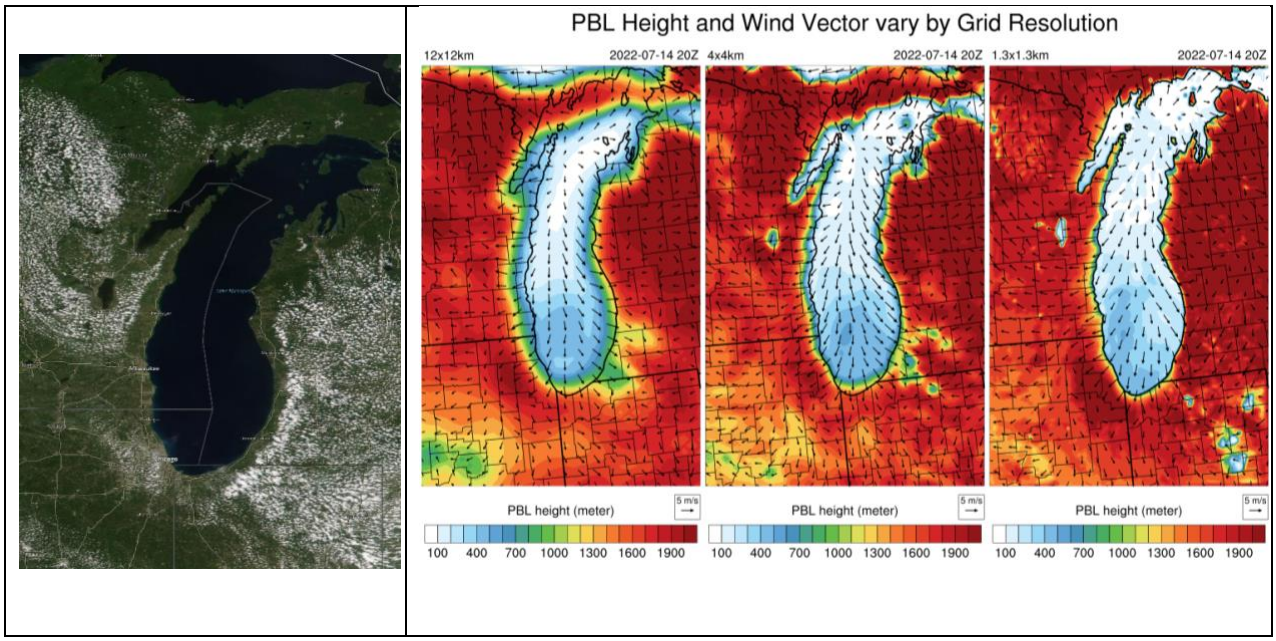

Figure 18. July 14, 2022 (14:00 CST) satellite imagery and modeled PBL height and wind vectors

For the three lake breeze case studies presented here, WRF successfully reproduced the surface flow convergence zone inland from the lakeshore, seen as the higher inland PBL heights in the figures above. The finer grid (4 km and 1.3 km) WRF resolutions also successfully resolved some of the small to mid-scale convective processes, i.e., the small clusters of lower PBL heights indicate the formation of fair-weather cumulus clouds over the land. These clouds are a common feature of lake-breeze fronts, as seen in the true color satellite imagery. Quantitative WRF model performance at simulating the lake-breeze is discussed in the following sections.

4.3 CART Analysis for Lake-breeze Events

4.3.1 Meteorological conditions of lake-breezes in Lake Michigan shoreline

Figure 19 lists the meteorological conditions that CART associated with lake-breeze days along the west and east shorelines of Lake Michigan. As 'lake-breeze' at Lake Michigan shores is a definite variable to indicate air flow from lake to land, CART identifies wind direction as the first branching variable in its classification. The graduated red and blue colored tree nodes (or clusters) at the bottom of the classification tree identify the meteorological conditions associated with lake-breeze events (and non-lake-breeze events such as land-breezes).

The CART analysis identified the top five most important variables for capturing lake-breeze events at the Racine, WI (KRAC) station in the following order of importance: temperature, specific humidity, wind direction, hourly change in specific humidity, and wind speed. The analysis revealed that lake-breezes at this station typically occurred during hot and humid summer afternoons, with three distinct wind directions observed. These variations in wind direction depended on the location of the wind convergence formed over Lake Michigan.

- Warm and moist air mass with northerly wind (temperature ranges in 22-24°C and specific humidity > 9.8 g/kg)
- Hot and humid air mass with NNE to ESE wind (temperature >22°C, specific humidity is >9.8 g/kg, wind direction ranges in 14-144°)
- Hot and moderate air mass coming from ESE to SSE direction (temperature >22°C, specific humidity is >9.8 g/kg, wind direction ranges in 124-144°)

The CART analysis identified the top five most important variables for capturing lake-breeze events at the Muskegon, MI (KMKG) station in the following order of importance: temperature, wind direction, specific humidity, wind speed, and hourly change in specific humidity. The CART analysis identified two distinct meteorological conditions associated with lake-breeze noted at the Muskegon station.

- Warm and moist air mass with southeasterly wind (temperature ranges in 23-25°C and specific humidity ranges in 15-19 g/kg)
- Hot air mass with south-southwesterly to north-northwesterly calm wind (temperature ranges in 25-29°C, wind speed <5 m/s, wind direction ranges in 208-330°) with notable changes in hourly temperature (0.3-1.1°C/hour) and slight to significant shifts in wind direction (10-30°/hour).

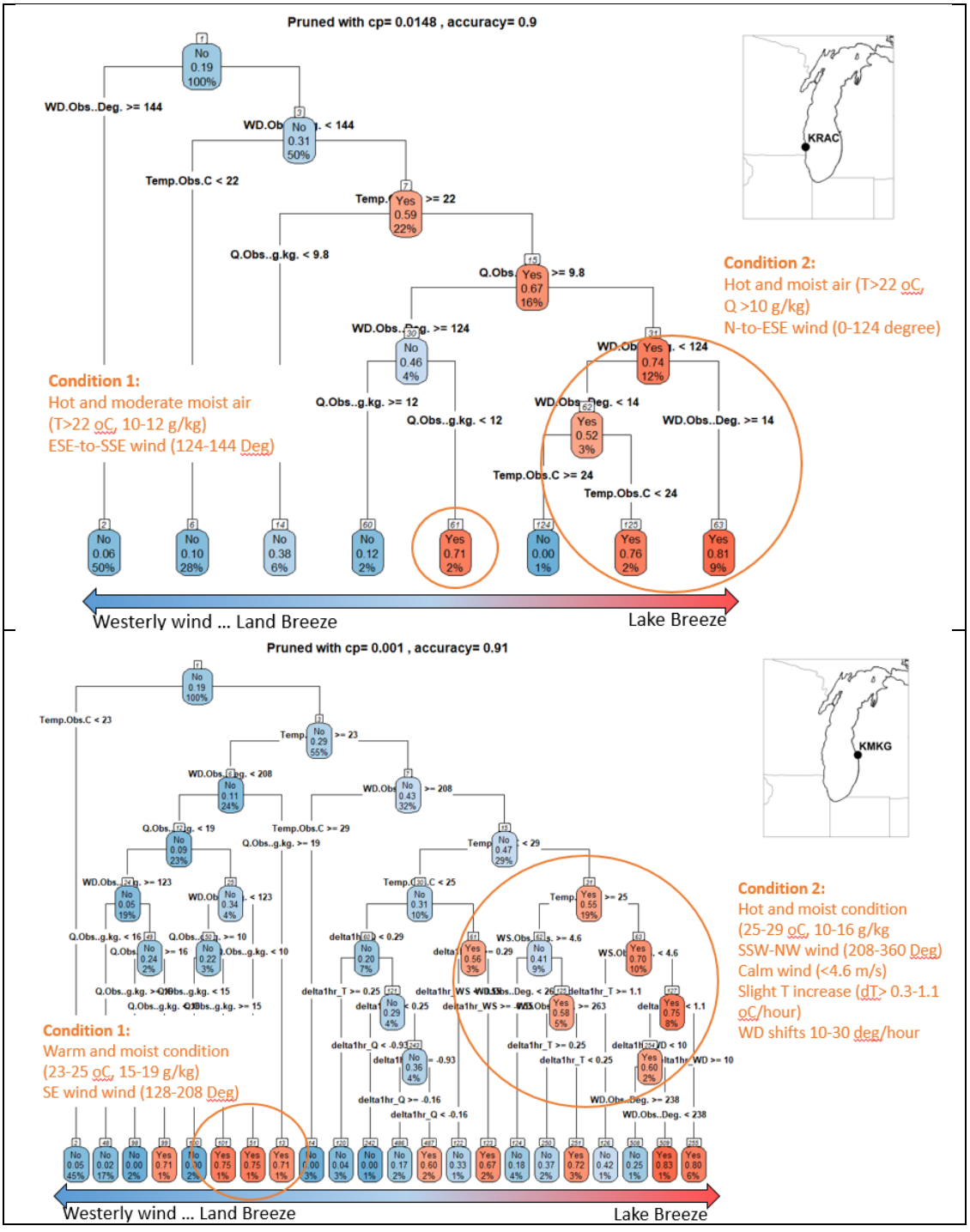

Figure 19. Meteorological conditions classified during the lake-breeze periods at western shoreline (KRAC station on the top) and eastern shoreline (KMKG station on the bottom) of Lake Michigan during 12-16 CDT, summer 2022. Graduated red and blue colored tree nodes indicate strength of predicted probability of the lake-breeze events and offshore flows.

Table 12 summarizes the typical meteorological conditions and hourly indicators of lake-breeze events for the western and eastern shores of Lake Michigan. In the western shore of Lake Michigan, the lake-breeze sets in during warm, moderately humid, and northeast-to-southeasterly wind conditions. During this condition, wind direction shifts in 10-40 degrees from previous hour record, with slight wind speed increase (0.5-1.0 m/s per hour), temperature drop (0.3-1.2^{o} C per hour), and specific humidity increase (0.3-0.8 g/kg per hour) during 12:00-16:00 CDT.

Westerly flow is the dominant meteorological condition for lake-breeze events along the eastern shore of Lake Michigan. Other conditions include hourly wind direction changes in the range of 10-20°, and slight drops in wind speed (0.5-1.0 m/s) during the onset of a lake-breeze. The lake-breeze occurs in much warmer and more humid conditions in the east shore of Lake Michigan (T>23-29^{o}C and 10g/kg<Q<19 g/kg) as compared to the west shore (T >19-30^{o}C and 8g/kg<Q<15 g/kg). There are two METAR stations (KGYY and KIGQ) located on the south end of the lake, however, the CART trees were not produced due to insufficient data samples in 2022.

Table 12. Classified meteorological conditions for lake-breeze events in Lake Michigan basin during 12-16 CDT, summer of 2022

West shoreline (5 stations)	East shoreline (5 stations)
Meteorological conditions during the lake-breeze events	
19°C< Temp < 30°C	Temp >23-29°C
8 g/kg < Humidity < 15 g/kg	10 g/kg < Humidity <19 g/kg
0.5-2.5 m/s < Wind speed <6.7 m/s	3.6 m/s <Wind speed< 6.2 m/s
94 Deg <Wind direction <114-184 Deg	108-253 Deg <Wind direction <248-353 Deg
Hourly indicators for onset of lake-breeze	
Moderate temperature drop (0.25-1.2° C per hour)	Very slight temperature drop (0.6 °C per hour), followed by an increase
Moderate humidity increase (0.3-0.8 g/kg per hour)	Slight humidity increase (<0.3 g/kg per hour)
Slight wind speed increase (0.5-1.0 m/s per hour)	Slight wind speed decrease (0.5-1.0 m/s per hour)
Slight to greater wind direction shift (10-40 deg per hour)	Slight wind direction shift (10-20 deg per hour)

4.3.2 WRF model performance during lake-breeze events along the Lake Michigan shoreline

LADCO calculated model performance statistics using surface observations and WRF modeled values at ten shoreline stations on days when the CART-predicted lake-breeze probability was greater than 70%. We also calculated performance statistics at these stations on similar days, but

lake-breeze was not predicted through the CART regression to compare the WRF performances for lake-breeze and non–lake-breeze events. Table 13 presents the WRF mean absolute errors and mean biases on lake-breeze and non-lake-breeze days averaged across all three LADCO WRF grid resolution simulations (12/4/1.33 km) near Lake Michigan. WRF performs well at the shoreline stations for days with and without a lake-breeze, and under similar meteorological conditions. The model errors and biases are within the WRF performance benchmarks. The model performance for lake-breeze and non-lake-breeze days are minimal and comparable, wind direction was slightly degraded on lake-breeze days as compared to the non-lake-breeze case.

Table 13. Average WRF model performance summary for lake-breeze and non-lake-breeze days along the shoreline of Lake Michigan in 2022

Variable	**Lake-breeze** (n=150)		**Non-lake-breeze** (n =144)	
	MAE	**MB**	**MAE**	**MB**
Temp2m	1.3	-0.1	1.3	-0.1
MixingRatio2m	1.0	-0.4	1.0	-0.1
Wind speed10m	1.1	-0.4	1.2	-0.5
Wind direction10m	22.5	-1.2	20.1	1.1

Table 14 presents WRF performance statistics for lake-breeze days across different model grid resolutions. Refinement to the model grid resolution does not produce a significant performance improvement. Temperature, specific humidity, and wind speed errors for all grid resolutions are in a range of 0.9-1.5; and wind direction errors in a range of 20.1-26.7 degrees. The WRF temperature forecasts for the finer 4-km and 1.3-km grids have the lowest error, while the 12-km grid simulation tends to have 0.5^{o}C higher errors on an average during the lake-breeze events. Both specific humidity and wind speed are slightly underestimated by about 0.4 in respective measured values on the 12-km and 4-km grid resolutions. The 1.3-km grid performance errors are comparable with the coarse grids for all examined variables, except for the wind direction having higher errors.

Table 14. Average WRF 2022 model performance summary by model grid resolution for the lake-breeze events in the shoreline of Lake Michigan

Variable	12 km		4 km		1.3 km	
	MAE	MB	MAE	MB	MAE	MB
Temp2m	1.5	-0.6	1.1	-0.2	1.2	0.3
MixingRatio2m	1.1	-0.5	0.9	-0.2	1.0	-0.5
Wind speed10m	1.1	-0.5	1.0	-0.4	1.1	-0.5
Wind direction10m	20.6	-0.9	20.1	-2.6	26.7	3.0

In addition, station specific WRF model errors and biases for the lake-breeze and non-lake-breeze events are show in Figure 20 and Figure 21, respectively. The box-and-whisker plots summarize the performance across all three grids for lake-breeze and non-lake-breeze days, while the dots show the performance statistics for each grid resolution within the lake-breeze groupings. The light gray lines in each panel represent the model performance benchmark values for each variable, as defined by Emery et al. (2001).

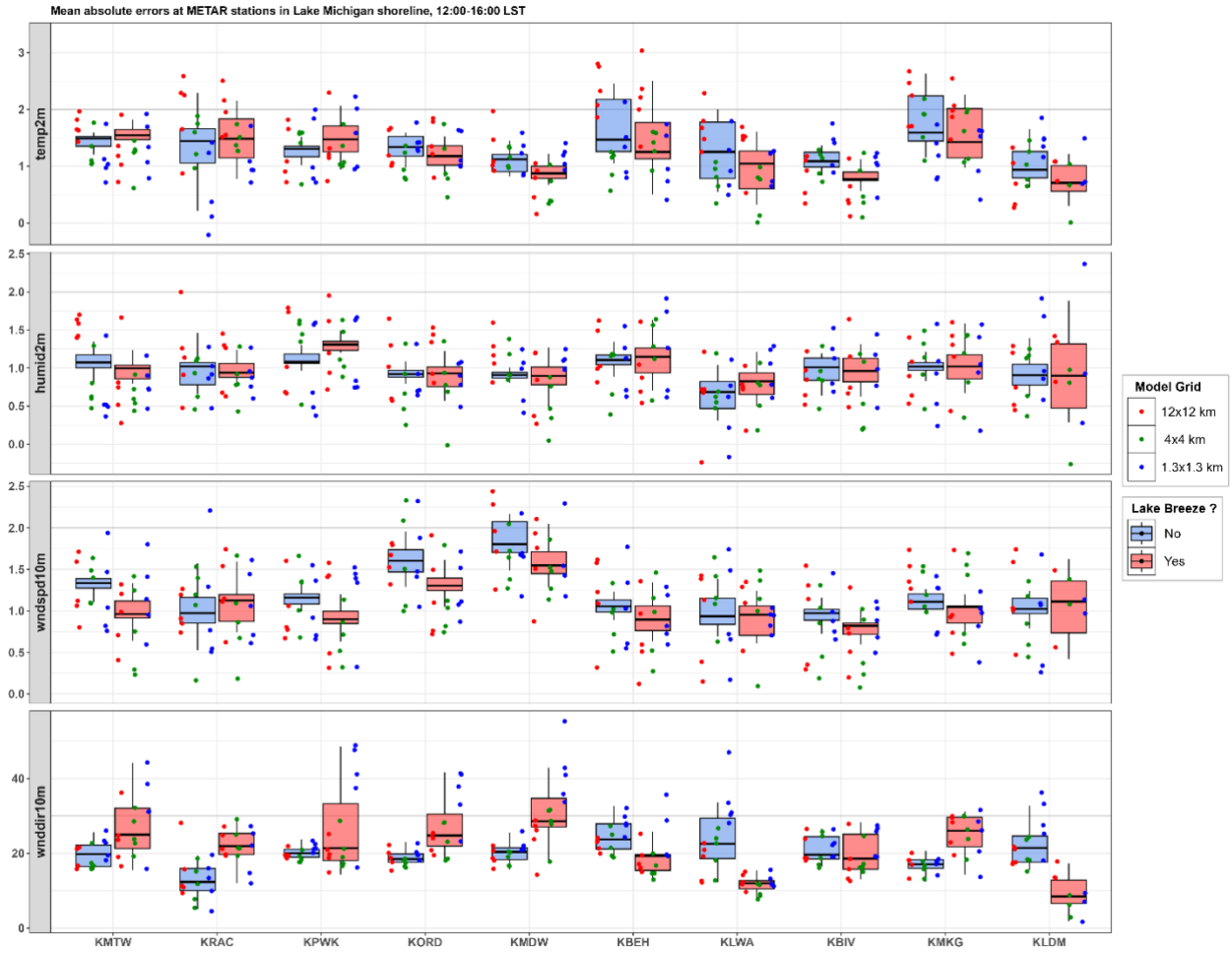

Figure 20. Mean absolute errors for temperature, specific humidity, wind speed and direction at METAR stations in Lake Michigan shore.

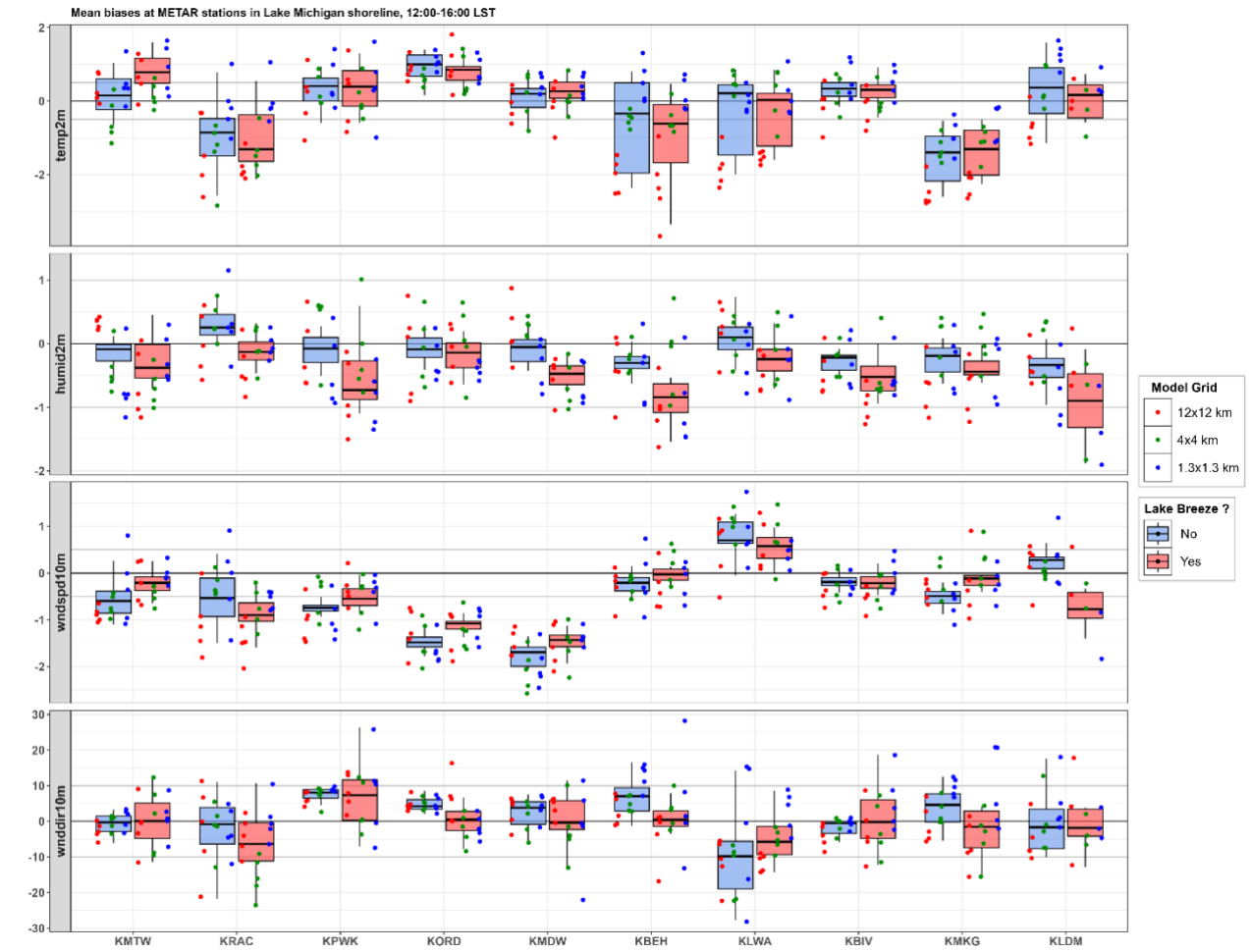

Figure 21. Mean biases for temperature, specific humidity, wind speed and direction at METAR stations in Lake Michigan shore

Model absolute errors for temperature, specific humidity, and wind speed at three stations located in the northwestern shore of Lake Michigan (KMTW, KRAC, and KPWK) tend to be slightly higher than those in the southwest and east shore of the lake (see first three stations in Figure 20). The wind direction errors are higher on the west shoreline (27 degrees), and much lower on the east shore of the lake (20 degrees) during the lake-breeze days. The mean bias box-and-whisker plot (Figure 21) shows that model biases for examined variables tends to be reduced for the lake-breeze vs. non-lake-breeze days following the errors reduction trend, but no difference seen in biases when going from coarse to finer grid resolutions within the lake-breeze groups. At the southwest and eastern shore of Lake Michigan stations, model errors and biases for

temperature, specific humidity and wind speed are reduced during the lake-breeze days compared to the non-lake-breeze days.

The mean absolute errors averaged by all examined variables for lake-breeze days (Figure 22) show that model performances for all examined variables are significantly improved going from 12-km to 4-km grid resolution, but it worsened at the 1.3-km grid resolution. In general, the WRF simulation of the examined surface meteorological variables during lake-breeze events are within the commonly used performance benchmark for simple meteorological conditions and the performance statistics are even better for the lake-breeze days than those for non-lake-breeze days at majority of the examined stations.

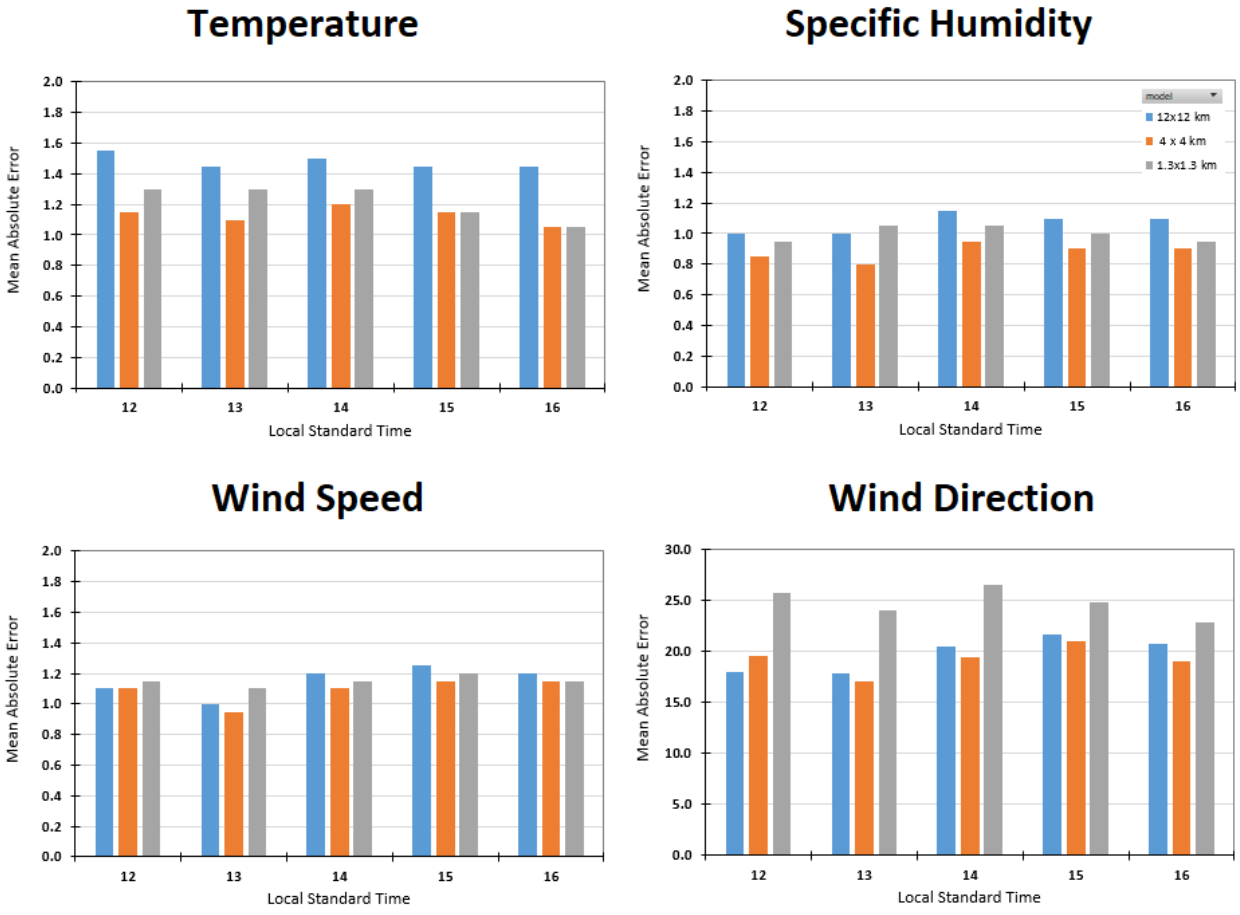

Figure 22. Mean absolute errors for temperature, specific humidity, wind speed and direction during lake-breeze afternoon hours, summer 2022, aggregated by model grid resolution

4.4 Lake-breeze Performance Summary

Accurate knowledge of WRF model performance during the lake-breeze events is needed to understand and anticipate its impact on simulating surface ozone concentrations in the Great Lakes Basin, especially near the shorelines of the lakes. Qualitative comparison of WRF modeled PBL height and wind fields with the lake-breeze front identified by satellite imagery and observed wind fields revealed that WRF successfully reproduced lake-breeze conditions and the associated inland surface convergence zones during selected high ozone days in 2022. Local scale convective processes were better resolved by the 4km and 1.33 km grid resolutions, which lead to better simulations of the land and lake circulation near the lake shores.

LADCO identified lake-breeze days during summer 2022 using satellite imagery, radar imagery, and NOAA's GFS model wind fields to visualize lake-breeze fronts and surface convergence zones. The identified days were used to develop a CART statistical model using data from selected METAR surface stations on the shoreline of Lake Michigan for predicting lake-breeze days. The CART model regression and classification accuracies for lake-breeze days were 92% for Lake Michigan on average. LADCO used the CART model to determine the typical meteorological conditions and indicators for lake-breeze days along the shores of Lake Michigan, and then used the model to identify all lake breeze days during April through October 2022.

LADCO calculated WRF model performance for lake-breeze and non-lake-breeze days. WRF performed well predicting temperature, humidity, and winds at the shoreline stations of Lake Michigan. The WRF model errors and biases for temperature, specific humidity, wind speed, and wind direction are well within the performance benchmarks for simple meteorological conditions, particularly along the southwest and eastern shores of Lake Michigan. The model performance is slightly better on the lake-breeze days compared to the non-lake-breeze days at most of stations examined. While errors and biases were significantly reduced on lake-breeze days at the 4-km grid resolution (MAEs are 1.1K for temperature, 0.9 g/kg for specific humidity, 1.1 m/s for wind speed, and 20 degrees for wind direction), they worsened slightly at the 1.3-km grid resolution near the Lake Michigan shore.

5 Conclusions and Future Work (Zac)

5.1 Cumulative assessment for the 2022 WRF Model Estimates

LADCO simulated 2022 meteorology with the WRFv4.5 model on three nested domains that focus on the Great Lakes Basin. LADCO simulated annual 2022 meteorology for an outer continental U.S. 12-km domain and the inner 4-km domain, and the ozone season (April – October) for the innermost 1.33-km nested domain. LADCO used physics and initialization options identified as the best performing WRF configuration in the LADCO region through a series of model configuration sensitivity experiments.

The LADCO 2022 WRF simulation is in good agreement with observations of surface meteorological variables deemed important for simulating air quality. The WRF performance statistics for all grid resolutions simulated by LADCO are within the acceptable meteorology model performance benchmarks proposed by Emery et al. (2001) and Kemball-Cook et al. (2005) for air quality model applications. The LADCO 2022 WRF simulation has a slight cool and wet bias in the summer months across much of the Eastern U.S. The model has a slight dry bias and warm bias in the winter season. The LADCO 2022 WRF configuration generally has the worst performance simulating conditions in the intermountain west.

LADCO compared summer season performance across the different grids that we simulated to evaluate how the model error and bias varies by grid resolution. The errors and biases in temperature and specific humidity predictions are reduced by about 10% in the 4-km resolution simulation compared to the 12-km simulation. The average model performance degraded at 1.33 km resolution relative to the 4-km results. The 1.33 km grid domains did resolve well local scale convective processes and had better performance (specifically, lower errors in wind direction) during the afternoon hours on days when lake-breeze conditions were observed.

LADCO assessed model performance during lake-breeze events using an approach developed to evaluate the LADCO 2016 WRF modeling (LADCO, 2022). We used a CART-based statistical model to identify typical meteorological conditions and hourly indicators for lake-breeze days, and then evaluated the model performance during lake-breeze conditions. We found that WRF performs relatively well in simulating conditions along the shorelines of Lake Michigan. WRF performance was slightly better on the lake-breeze days compared to the non-lake-breeze days.

5.2 Lesson Learned and Future Work

LADCO developed a WRF configuration for simulating 2022 air quality in the Great Lakes region. The combination of WRF APX physical parameterization schemes, high resolution NAM and HRRRv4 reanalysis data for ICBC, and the FDDA scheme used in the LADCO 2022 WRF modeling (LADCO_WRF45_APX_NAM_HRRR6_obs) proved to be the best configuration for 12/4/1.33 km grid resolution modeling of the annual simulation.

LADCO changed the source of data for constraining lake/sea surface temperatures (SST) in the 2022 WRF modeling compared to the 2016 LADCO modeling. The 3-km HRRRv4 reanalysis data provided a refined, easy to access surface level meteorological condition in the Midwest, especially for the diagnostic SST field for the Great Lakes. Although there are alternative SST data sources, including the 1-km GHRSST and GLSEA SST, implementation of these datasets in WPS is hindered by the fact that the GHRSST system is primarily designed to measure ocean surface temperatures and not typically intended to provide accurate readings for large lakes such as the Great Lakes, which can have significantly different temperature profiles compared to the open ocean. In addition, there is no well-tested processing step for integrating the irregular shaped GLSEA SST dataset into WPS.

LADCO used the AMET software to calculate WRF model performance statistics. AMET statistics are derived from collated observation and modeled values at the grid cells in which observation stations are located. For consistency with EPA's attainment test methods for air pollution, which considers modeled advection errors, future work at LADCO may modify, test, and operationalize the core codes of AMET to support the calculation of meteorological performance statistics based on a matrix of grid cells surrounding a monitor, e.g., 3x3 cells surrounding the observation station for the 12-km grid resolution regional model.

The model performance evaluation for lake-breeze events using CART analysis is a novel approach. Our methods will be improved in future applications by increasing the number of predictor variables for lake-breeze events to better isolate synoptic scale processes that may have similar characteristics with lake-breezes (Laird et al. 2001). We will also attempt to consider varying durations of the lake-breeze by identifying lake-breeze start and end times (Wagner et al.

2022). We summarized WRF performance for the meteorological conditions that CART identified as lake-breeze days during 12:00-16:00 LST with the goal of having a consistent hour range regardless of the station location. Sills et al. (2007) indicated that lake-breeze conditions occurred between 10:00-20:00 LST along the shores of Lake Erie with durations of 2-13 hours depending on the weather condition. In future applications of the CART lake-breeze model LADCO will explore alternative periods during the diel for analyzing lake-breeze events.

References

Benjamin et al. 2016, A North American Hourly Assimilation and Model Forecast Cycle: The Rapid Refresh. Mon. Wea. Rev., 144, 1669-1694.

Breiman, L., J. Friedman, R. Olshen, and C. Stone, Classification and Regression Trees, Pacific Grove, CA: Wadsworth (1984).

Brook, J. R., Makar, P. A., Sills, D. M. L., Hayden, K. L., and McLaren, R.: Exploring the nature of air quality over southwestern Ontario: main findings from the Border Air Quality and Meteorology Study, Atmos. Chem. Phys., 13, 10461–10482, https://doi.org/10.5194/acp-13-10461-2013, 2013.

Campbell, P. C., Bash, J. O., and Spero, T. L.: Updates to the Noah land surface model in WRF-CMAQ to improve simulated meteorology, air quality, and deposition. Journal of Advances in Modeling Earth Systems, 11, 231– 256. https://doi.org/10.1029/2018MS001422, 2019.

Case, J. L., Crosson, W. L., Kumar, S. V., Lapenta, W. M., & Peters-Lidard, C. D. (2008). Impacts of High-Resolution Land Surface Initialization on Regional Sensible Weather Forecasts from the WRF Model, *Journal of Hydrometeorology*, *9*(6), 1249-1266. Retrieved May 26, 2022, from https://journals.ametsoc.org/view/journals/hydr/9/6/2008jhm990_1.xml

Case, J. L., Kumar, S. V., Srikishen, J., & Jedlovec, G. J. (2011). Improving Numerical Weather Predictions of Summertime Precipitation over the Southeastern United States through a High-Resolution Initialization of the Surface State, Weather and Forecasting, 26(6), 785-807. Retrieved May 26, 2022, from https://journals.ametsoc.org/view/journals/wefo/26/6/2011waf2222455

Cintineo, R., Otkin, J. A., Kong, F., and Xue, M.: Evaluating the accuracy of planetary boundary layer and cloud microphysical parameterization schemes in a convection-permitting ensemble using synthetic GOES-13 satellite observations, Mon. Wea. Rev., 142, 163-182, 2014.

Chen, F., and Dudhia, J.: Coupling an advanced land-surface/hydrology model with the Penn State/NCAR MM5 modeling system. Part I: Model description and implementation, Mon. Wea. Rev., 129, 569-585, 2001.

Dowell, D. C., and Coauthors, 2022: The High-Resolution Rapid Refresh (HRRR): An Hourly Updating Convection-Allowing Forecast Model. Part I: Motivation and System Description. Wea. Forecasting, 37, 1371–1395, https://doi.org/10.1175/WAF-D-21-0151.1.

Emery, C., E. Tai, and G. Yarwood, 2001. “Enhanced Meteorological Modeling and Performance Evaluation for Two Texas Ozone Episodes.” Prepared for the Texas Natural Resource Conservation Commission, prepared by ENVIRON International Corporation, Novato, CA. 31-August. http://www.tceq.texas.gov/assets/public/implementation/air/am/contracts/reports/mm/EnhancedMetModelingAndPerformanceEvaluati on.pdf

Ek, M. B., and Coauthors: Implementation of Noah land surface model advances in the National Centers for Environmental Prediction operational mesoscale Eta model, J. Geophys. Res., 108, 8851, doi:10.1029/2002JD003296, 2003.

Harkey, M., and Holloway, T.: Constrained dynamical downscaling for assessment of climate impacts, J. Geophys. Res. Atmos., 118, 2316-2148, doi: 10.1002/jgrd.50223, 2013.

Hong, S-Y., Y. Noh, Y., and J. Dudhia, J.: A new vertical diffusion package with explicit treatment of entrainment processes. Mon. Wea. Rev., 134, 2318–2341, doi: 10.1175/MWR3199.1, 2006.

Hong, S.-Y.: A new stable boundary-layer mixing scheme and its impact on the simulated East Asian summer monsoon, Quart. J. Roy. Meteor. Soc., 136, 1481–1496, 2010.

Griffin, S. M., and Coauthors: Evaluating the impact of planetary boundary layer, land surface model, and microphysics parameterization schemes on upper-level cloud objects in simulated GOES-16 brightness temperatures. J. Geophys. Res. - Atmos, 126, e2021JD034709. https://doi.org/10.1029/2021JD034709, 2021.

Kain, J.S.: The Kain-Fritsch convective parameterization: An update, J. Appl. Meteorol. Climatol., 43(1), 170-181, doi: 10.1175/1520-0450(2004)043<0170:TKCPAU>2.0.CO;2, 2004.

Kemball-Cook, S., Y. Jia, C. Emery, and R. Morris, 2005. Alaska MM5 Modeling for the 2002 Annual Period to Support Visibility Modeling. Prepared for the Western Regional Air Partnership, by ENVIRON International Corp., Nov

LADCO: 2022 Weather Research Forecasting Modeling Protocol for the LADCO States, 2024. https://www.ladco.org/wp-content/uploads/Modeling/2022/WRF/LADCO_WRF2022_ModelingProtocol_20June2024_Final.pdf.

LADCO: Weather Research Forecasting 2016 Meteorological Model Performance Evaluation. 2022. https://www.ladco.org/wp-content/uploads/Modeling/2016/WRF/LADCO_2016WRF_Performance_22June2022.pdf.

LADCO: 2016 Weather Research Forecasting Modeling Protocol for the LADCO States, 2018. https://www.ladco.org/wp-content/uploads/Modeling/2016/WRF/LADCO_WRF2016_ModelingProtocol_Final.pdf

Morrison, H., Curry, J. A., and Khvorostyanov, V. I.: A new double-moment microphysics parameterization for application in cloud and climate models. Part 1: Description, J. Atmos. Sci., 62, 1665-1677, doi: 10.1175/JAS3446.1, 2005.

McNally, D. E., 2009. “12km MM5 Performance Goals.” Presentation to the Ad-hoc Meteorology Group. 25-June. http://www.epa.gov/scram001/adhoc/mcnally2009.pdf

Pleim, J. E.: A combined local and nonlocal closure model for the atmospheric boundary layer. Part 1: Model description and testing, J. Appl. Meteorol. Climatol., 46, 1383-1395, doi: 10.1175/JAM2539.1, 2007.

Pleim, J. E. and Gilliam, R.: An indirect data assimilation scheme for deep soil temperature in the Pleim-Xiu land surface model. J. Appl. Meteorol. Climatol., 48, 1362-1376, doi: 10.1175/2009JAMC2053.1, 2009.

Pleim, J. E., and Xiu, A.: Development of a land surface model. Part II: data assimilation, J. Appl. Meteorol. 42, 1811–1822. https://doi.org/10.1175/1520-0450(2003)042<1811:DOALSM>2.0.CO;2, 2003.

Schwab, D. J., Leshkevich, G. A., and Muhr, G. C.: Satellite measurements of surface water temperature in the Great Lakes: Great Lakes Coast Watch, Journal of Great Lakes Research, 18, 247– 258, 1992.

Skamarock, W.C., J.B. Klemp, J. Dudhia, D.O. Gill, M. Barker, M.G. Duda, X.-Y. Huang, W. Wang, and J.G. Powers, 2008: A description of the Advanced Research WRF version 3. NCAR Technical Note NCAR/TN475+STR

Sills, D. M. L., Brook, J. R., Levy, I., Makar, P. A., Zhang, J., and Taylor, P. A.: Lake-breezes in the southern Great Lakes region and their influence during BAQS-Met 2007, Atmos. Chem. Phys., 11, 7955–7973, https://doi.org/10.5194/acp-11-7955-2011, 2011.

Sutton, C., Hamill T. M., and Warner T. T.: Will perturbing soil moisture improve warm-season ensemble forecasts? A proof of concept, Mon. Wea. Rev., 134, 3174–3189, 2006.

Thompson, G., Field, P. R., Rasmussen, R. M., and Hall, W. D.: Explicit forecasts of winter precipitation using an improved bulk microphysics scheme. Part II: Implementation of a new snow parameterization, Mon. Wea. Rev., 136, 5095–5115, 2008.

Thompson, G., Tewari, M., Ikeda, K., Tessendorf, S., Weeks, C., Otkin, J., Kong, F.: Explicitly-coupled cloud physics and radiation parameterizations and subsequent evaluation in WRF high-resolution convective forecasts. Atmos. Res., 168, 92-104, doi:10.1016/j.atmosres.2015.09.005, 2016.

US EPA. 2024. Meteorological Model Performance for Annual 2022 Simulation WRF v4.4.2. Research Triangle Park, NC. https://www.epa.gov/system/files/documents/2024-03/wrf_2022_tsd.pdf.

US EPA, 2019. Meteorological Model Performance for Annual 2016 Simulation WRF v3.8. (EPA-454/R-19-010) United States Environmental Protection Agency.

.

Appendix A: Additional Materials

Additional LADCO WRF 2022 simulation MPE plots are available on the LADCO website:

https://www.ladco.org/technical/modeling-results/2022-wrf-modeling/

.

A.1 CONUS 12 WRF MPE Plots

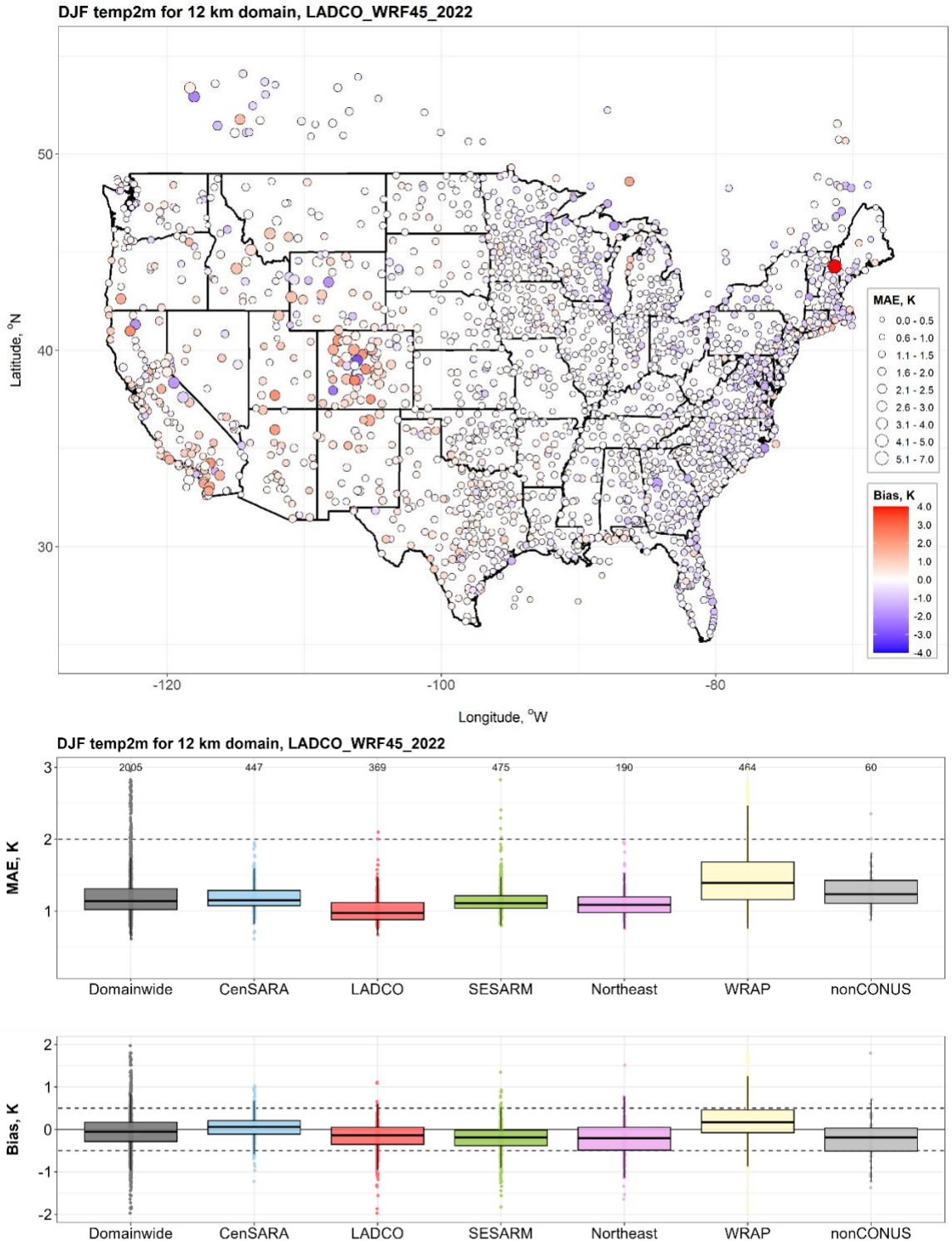

Figure 23. Mean Absolute errors and biases for 2-m temperature, the 12-km Domain, Winter 2022

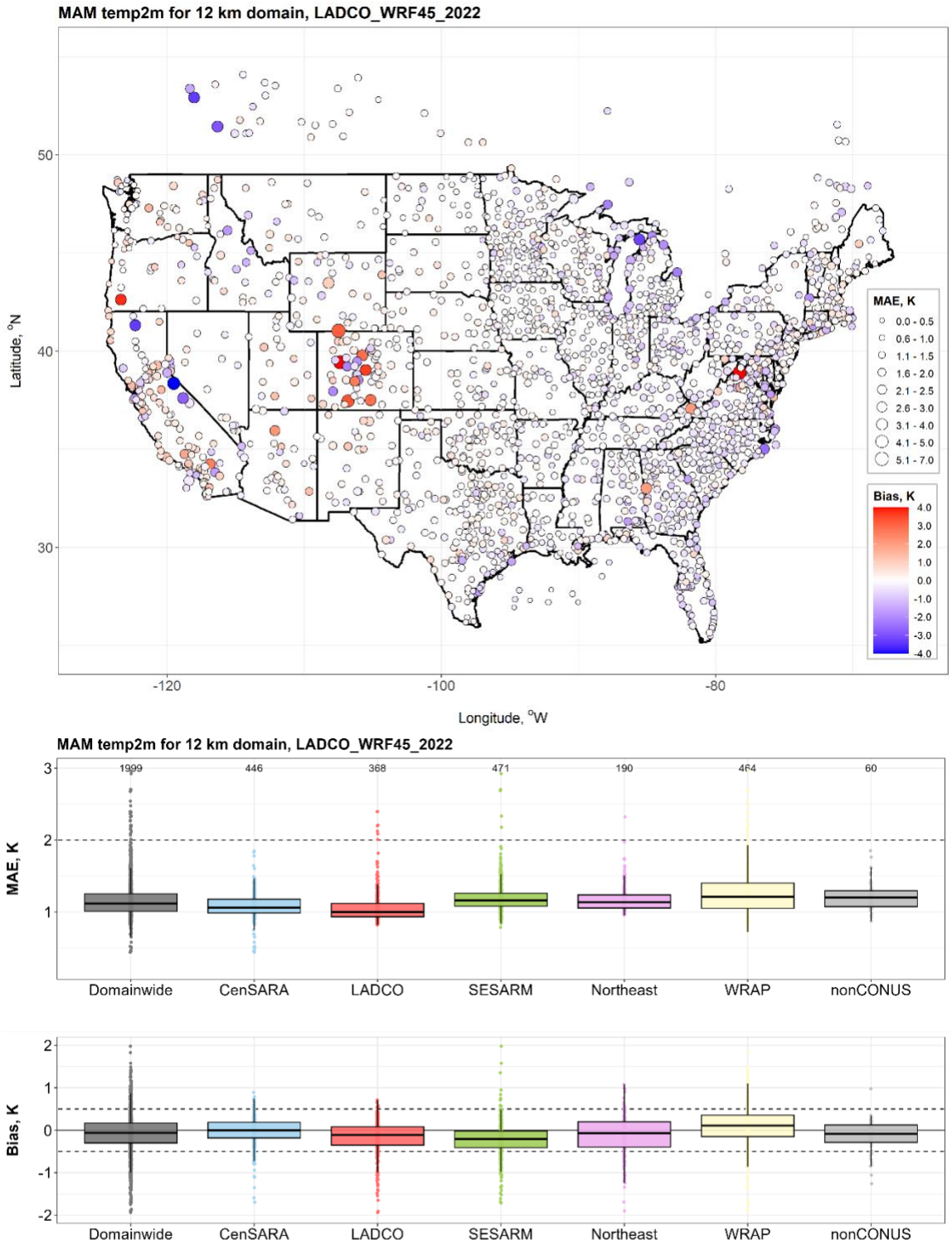

Figure 24. Mean Absolute Errors and Biases for Temperature, the 12-km Domain, Spring 2022

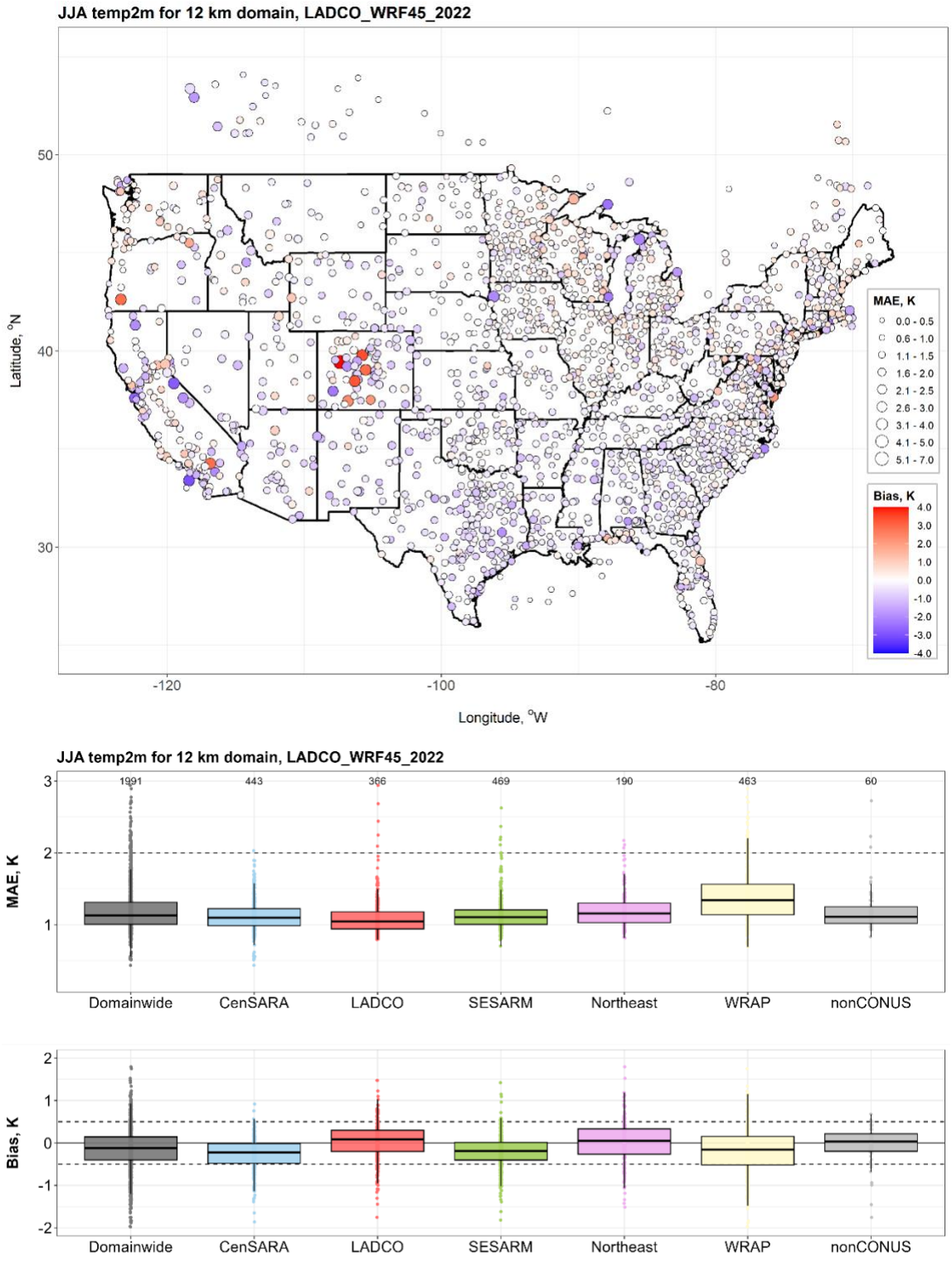

Figure 25. Mean Absolute Errors and Biases for Temperature, the 12-km Domain, Summer 2022

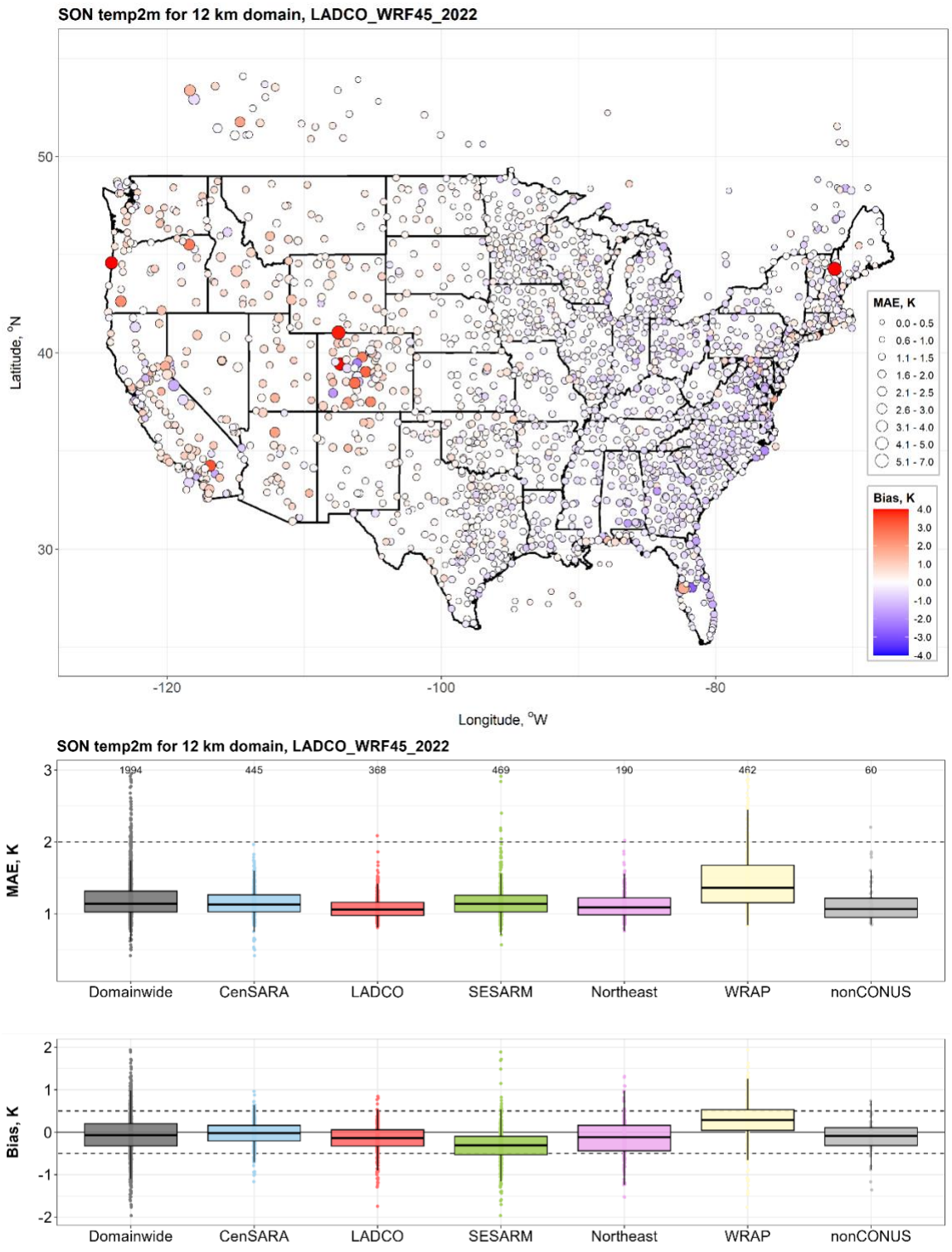

Figure 26. Mean Absolute Errors and Biases for Temperature, the 12-km Domain, Fall 2022

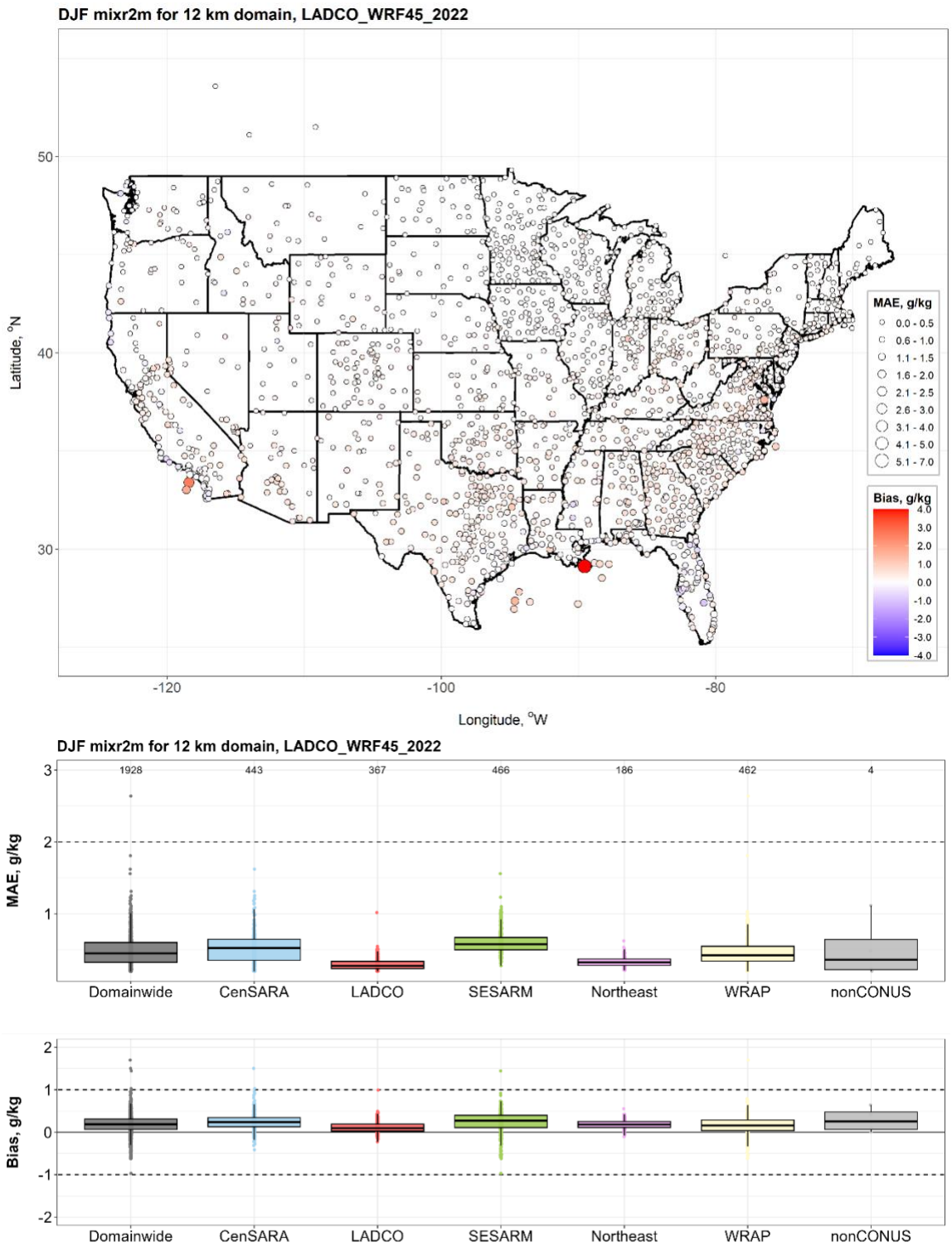

Figure 27. Mean Absolute Errors and Biases for Specific Humidity, the 12-km Domain, Winter 2022

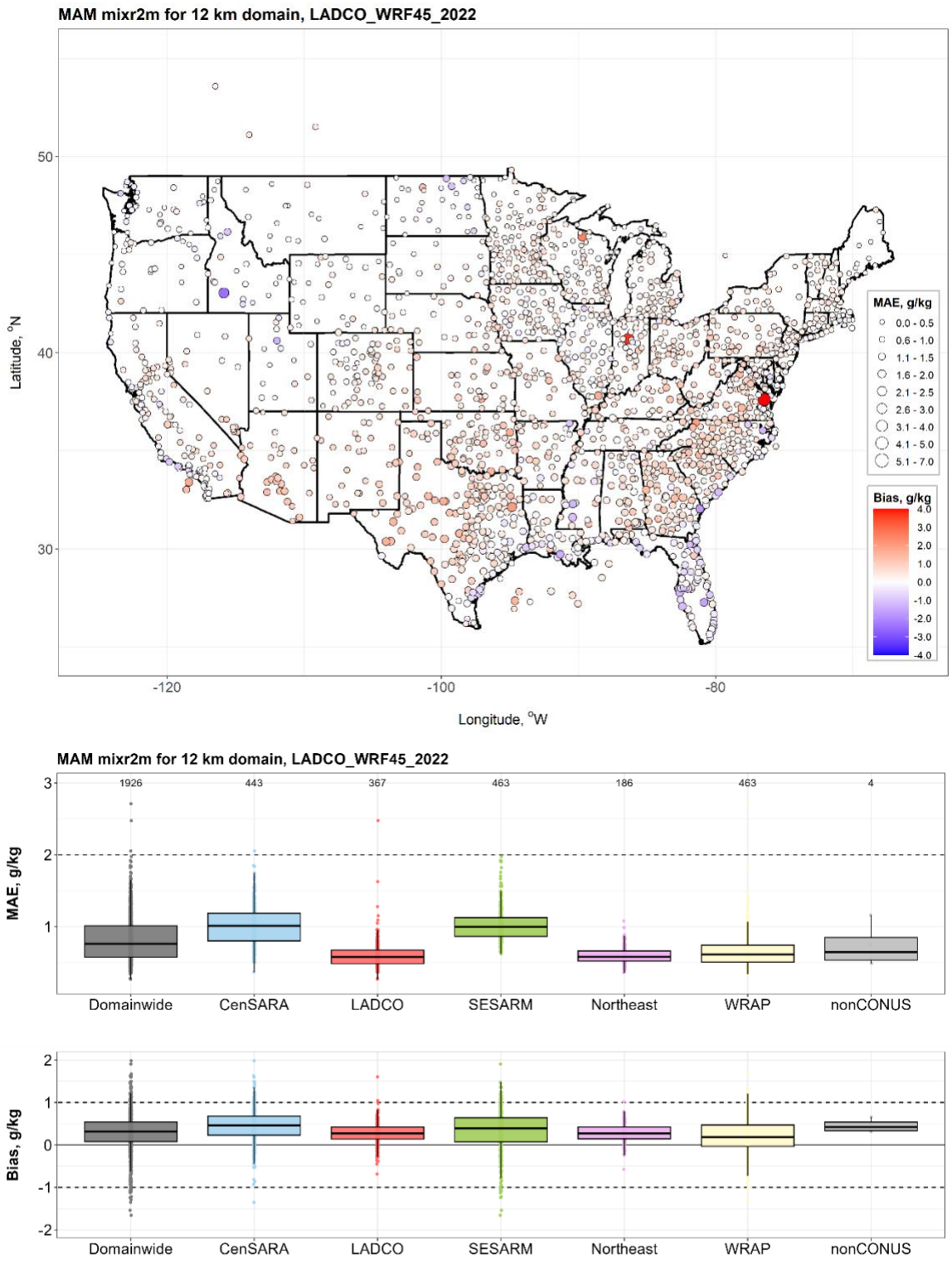

Figure 28. Mean Absolute Errors and Biases for Specific Humidity, the 12-km Domain, Spring 2022

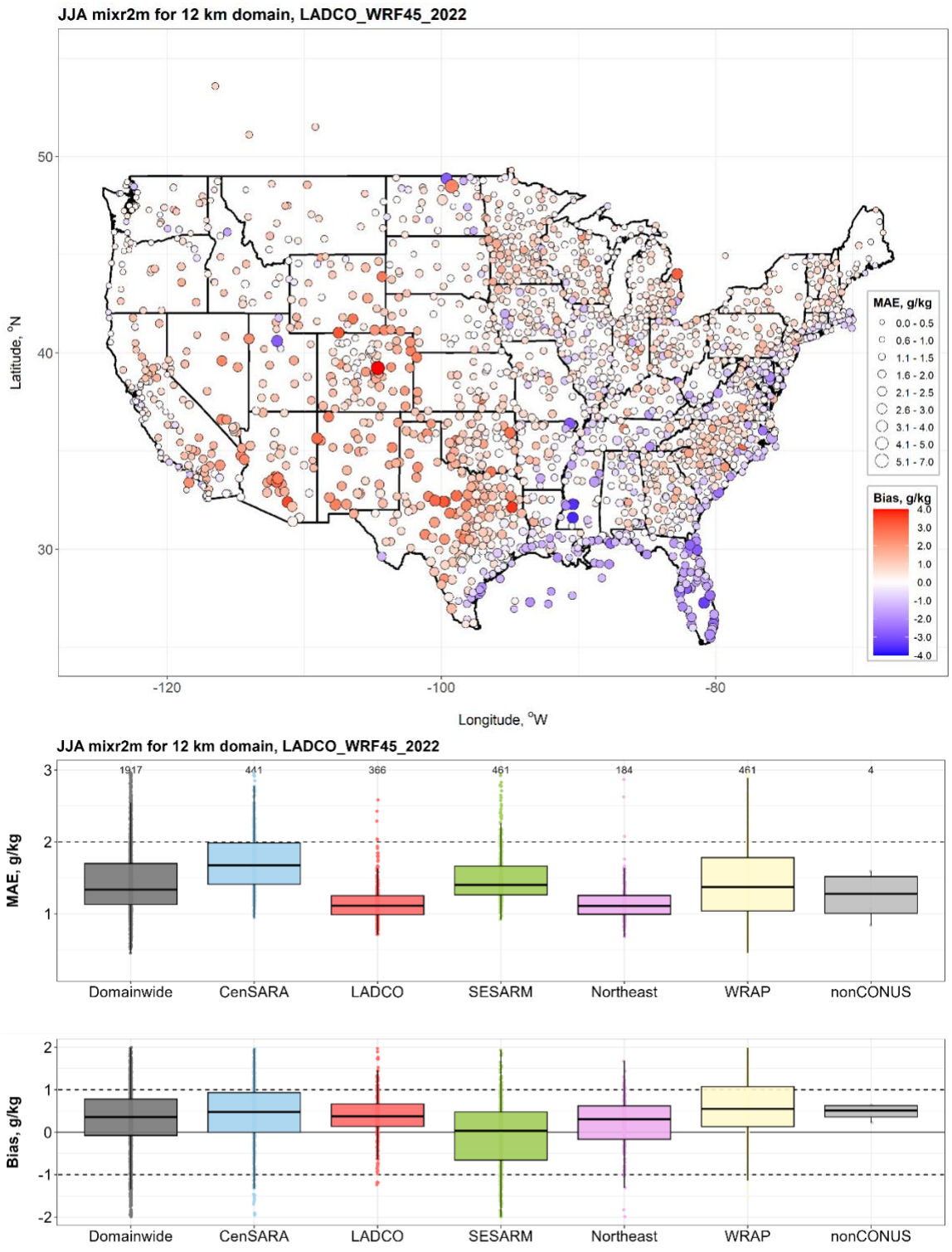

Figure 29. Mean absolute errors and biases for Specific Humidity, the 12-km Domain, Summer 2022

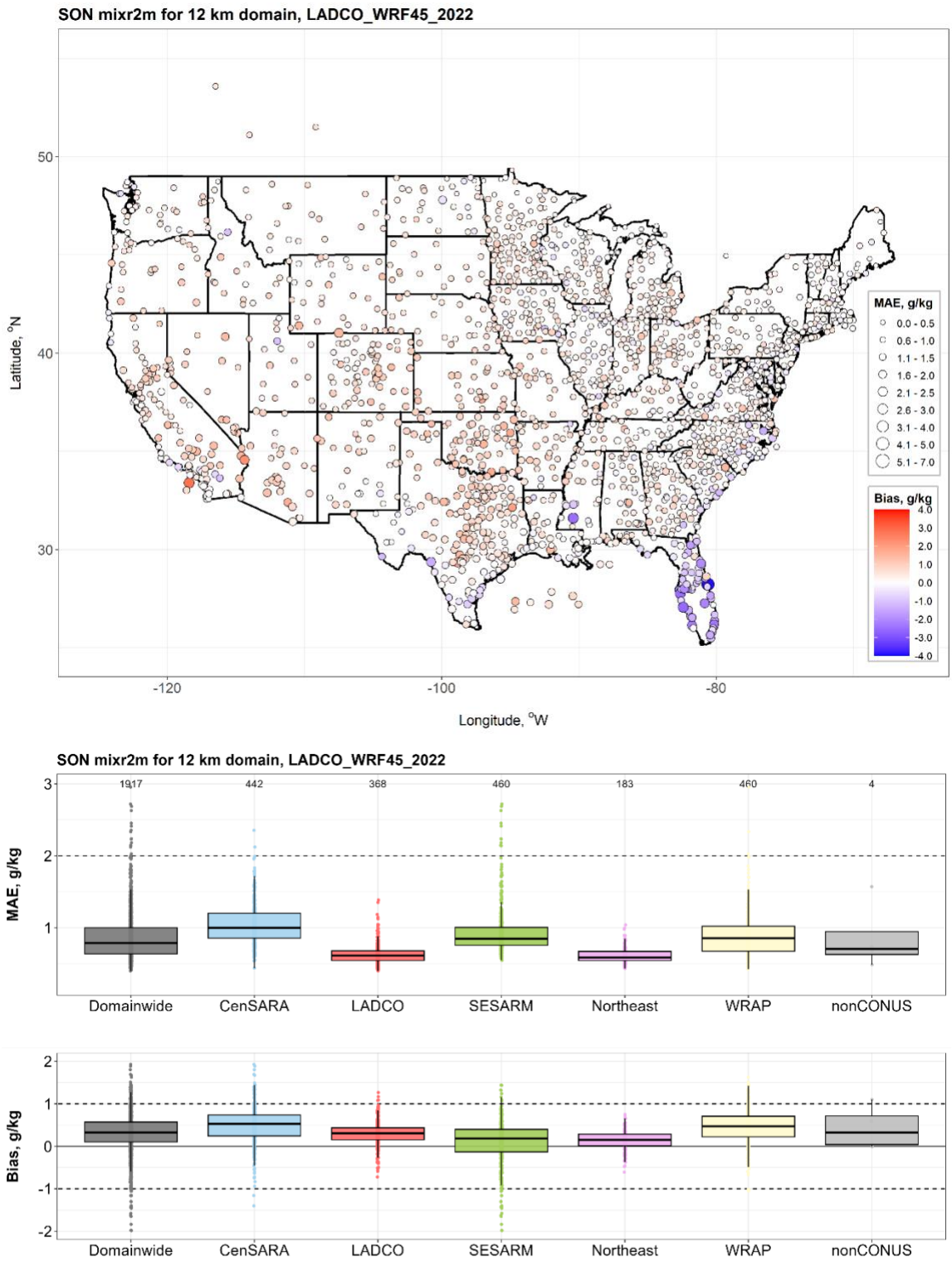

Figure 30. Mean Absolute Errors and Biases for Specific Humidity, the 12-km Domain, Fall 2022

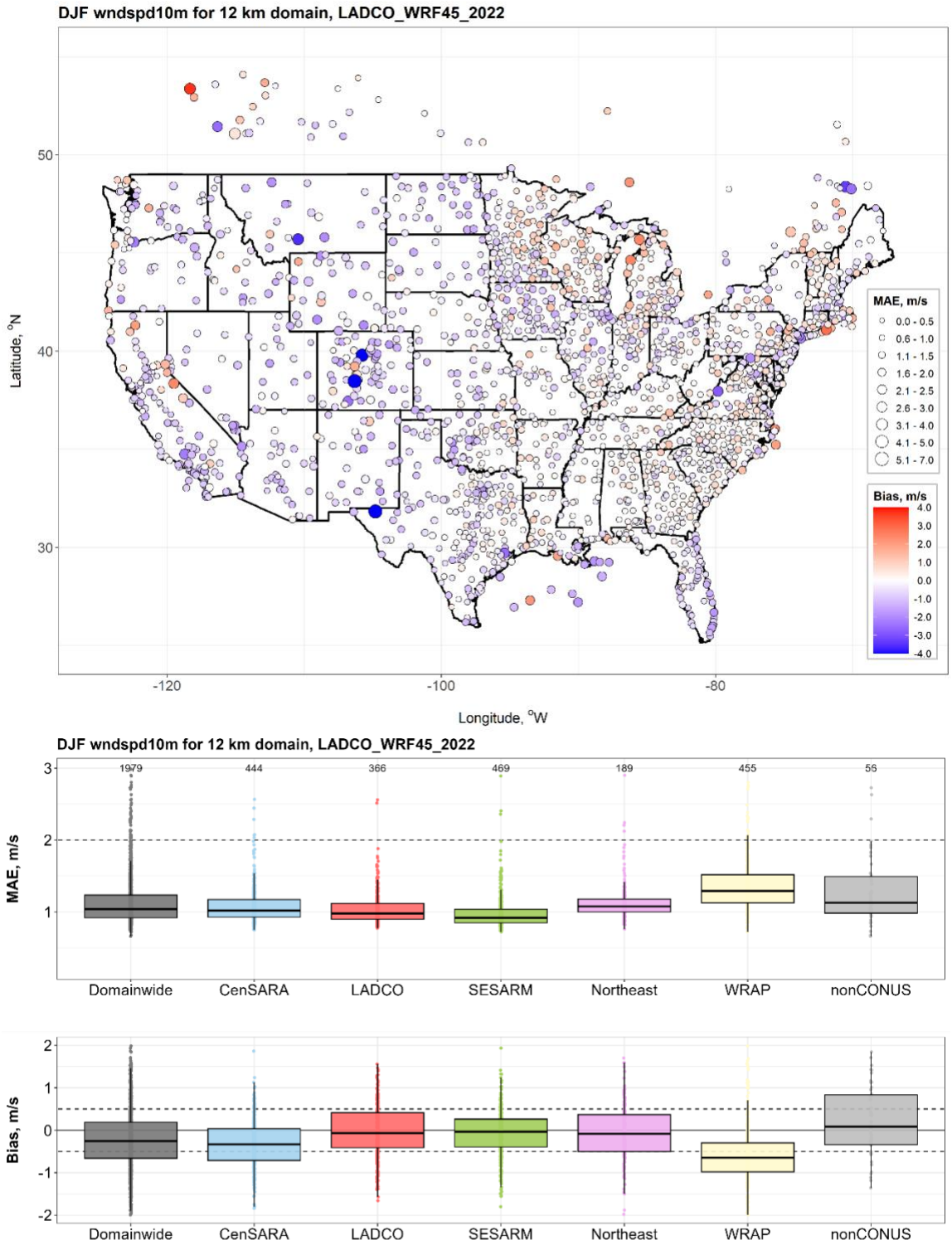

Figure 31. Mean Absolute Errors and Biases for Wind Speed, the 12-km Domain, Winter 2022

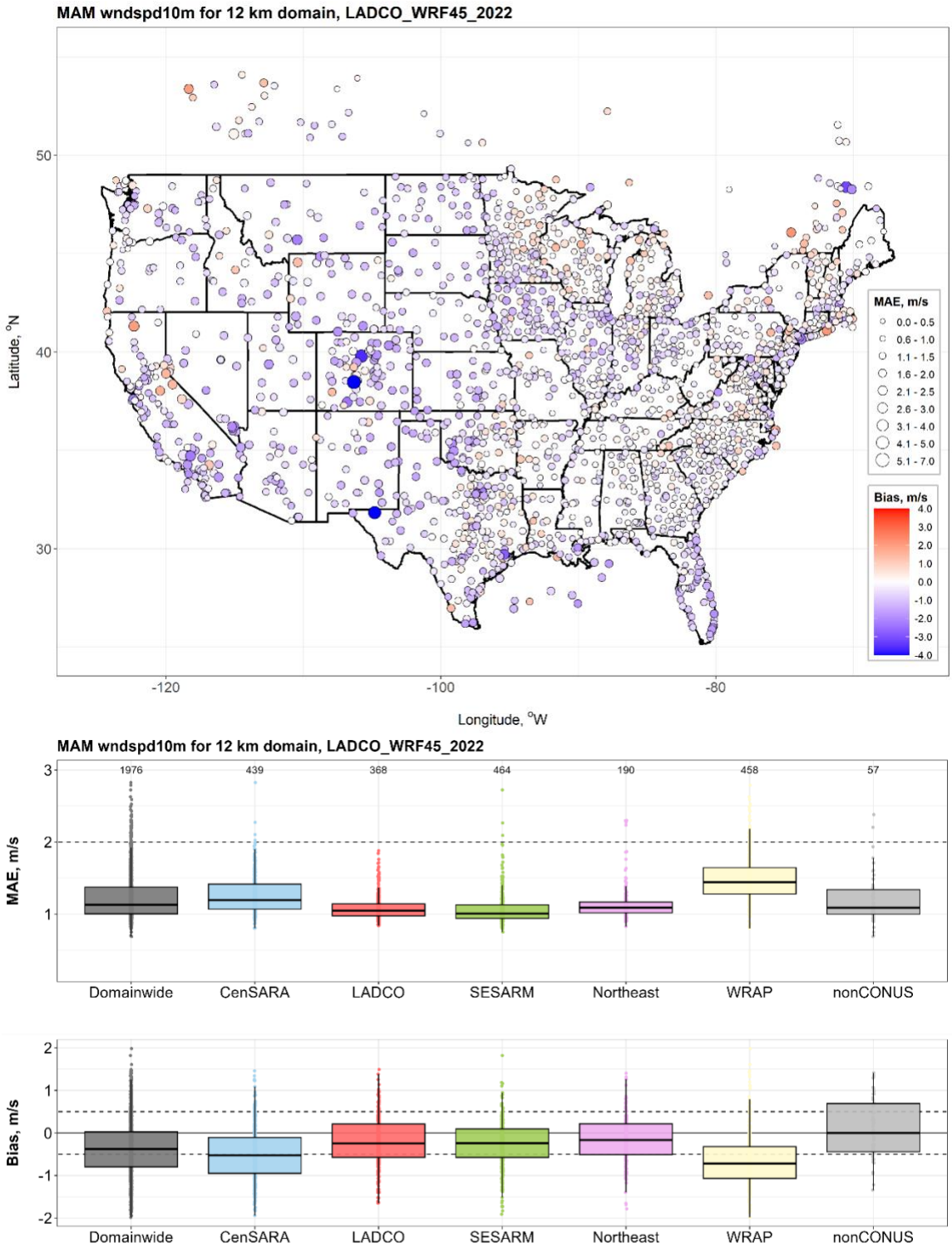

Figure 32. Mean Absolute Errors and Biases for Wind Speed, the 12-km Domain, Spring 2022

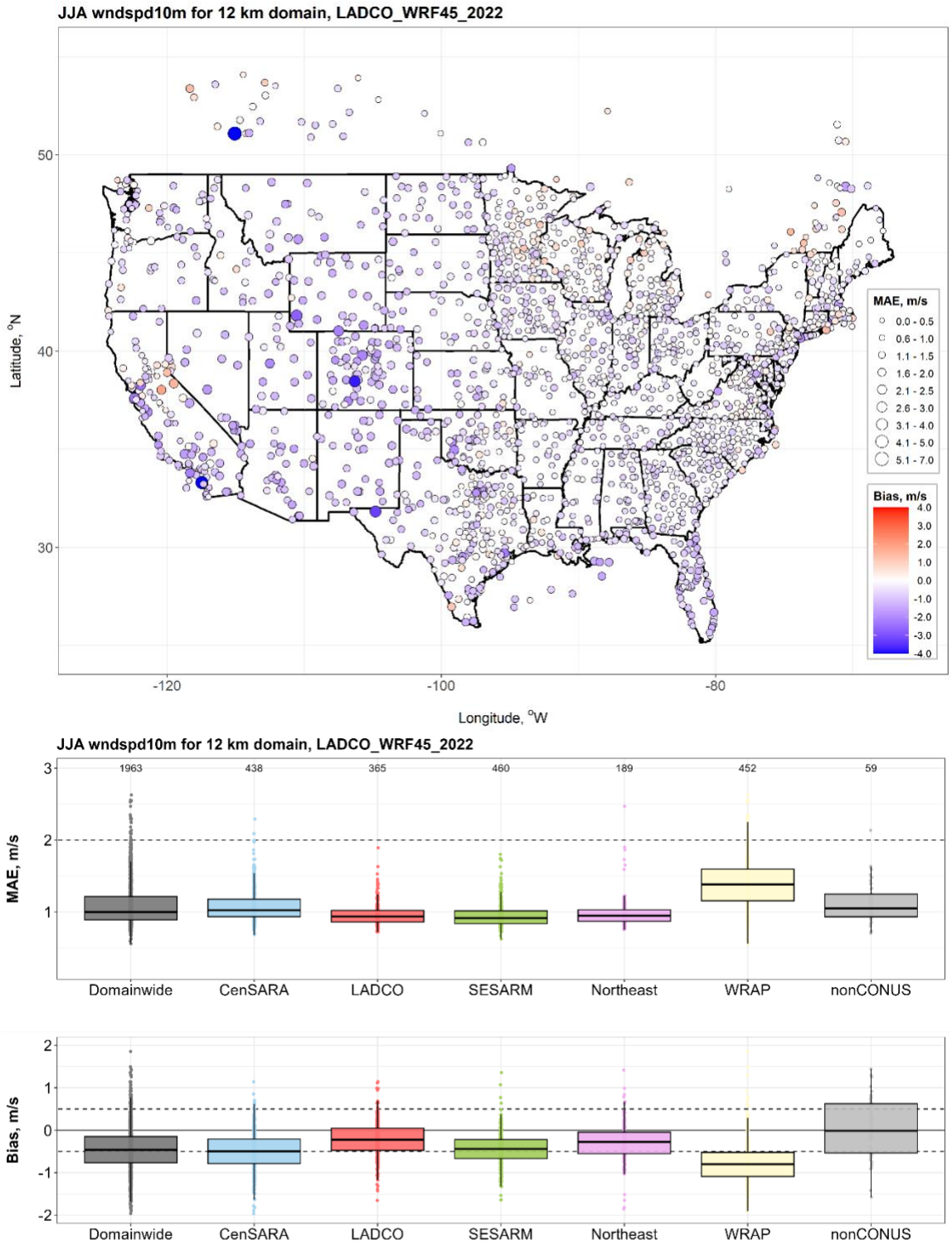

Figure 33. Mean Absolute Errors and Biases for Wind Speed, the 12-km Domain, Summer 2022

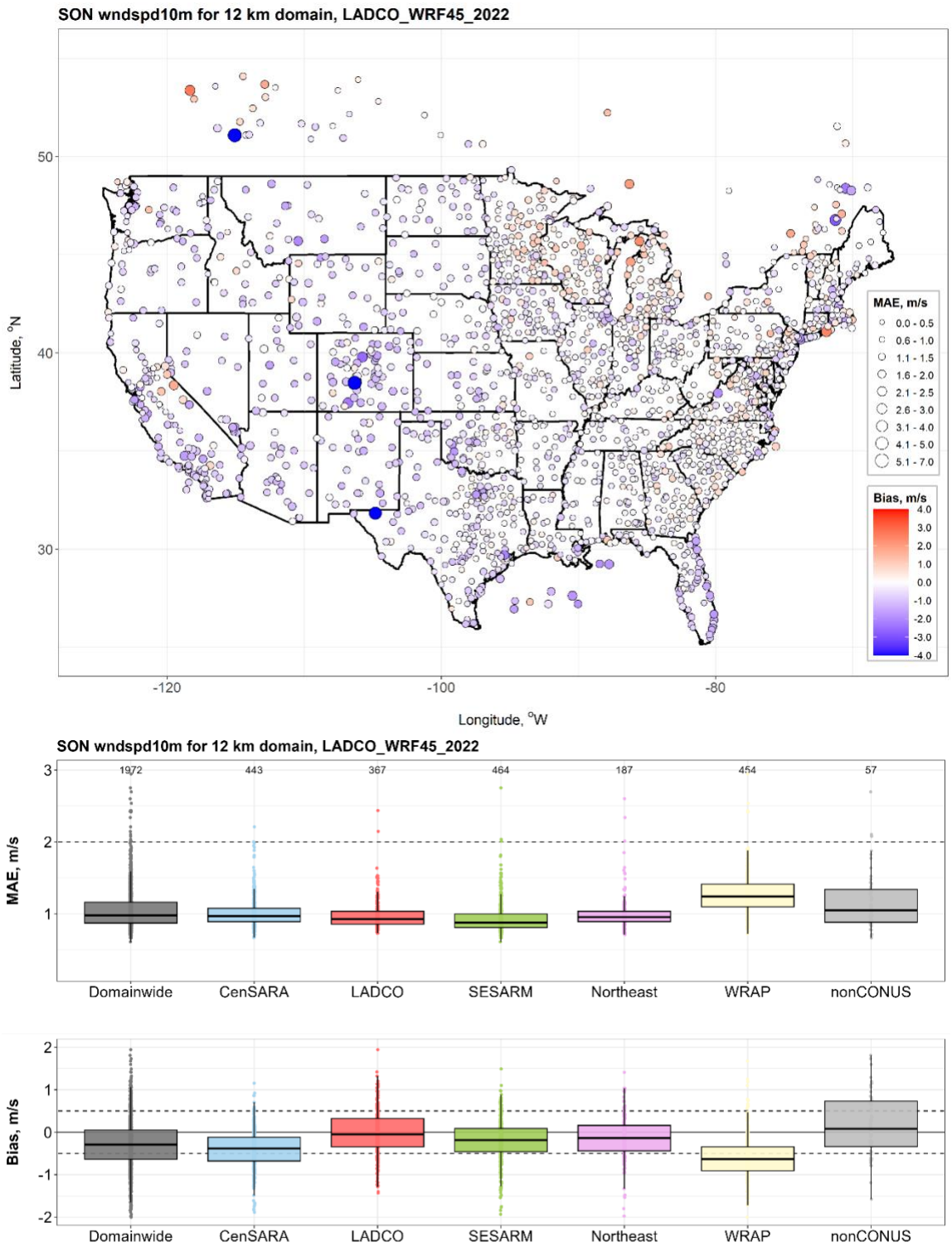

Figure 34. Mean Absolute Errors and Biases for Wind Speed, the 12-km Domain, Fall 2022

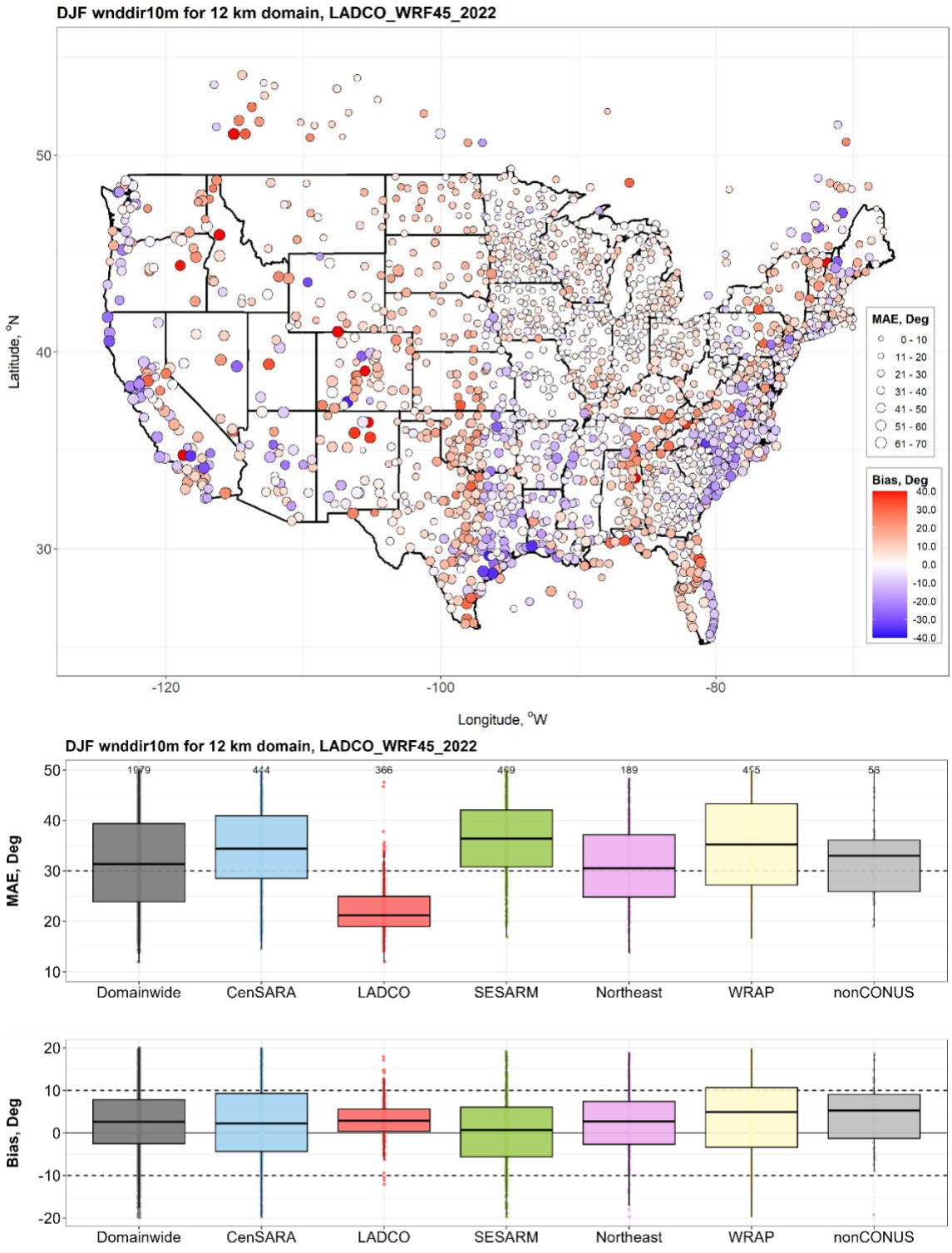

Figure 35. Mean Absolute Errors and Biases for Wind Direction, the 12-km Domain, Winter 2022

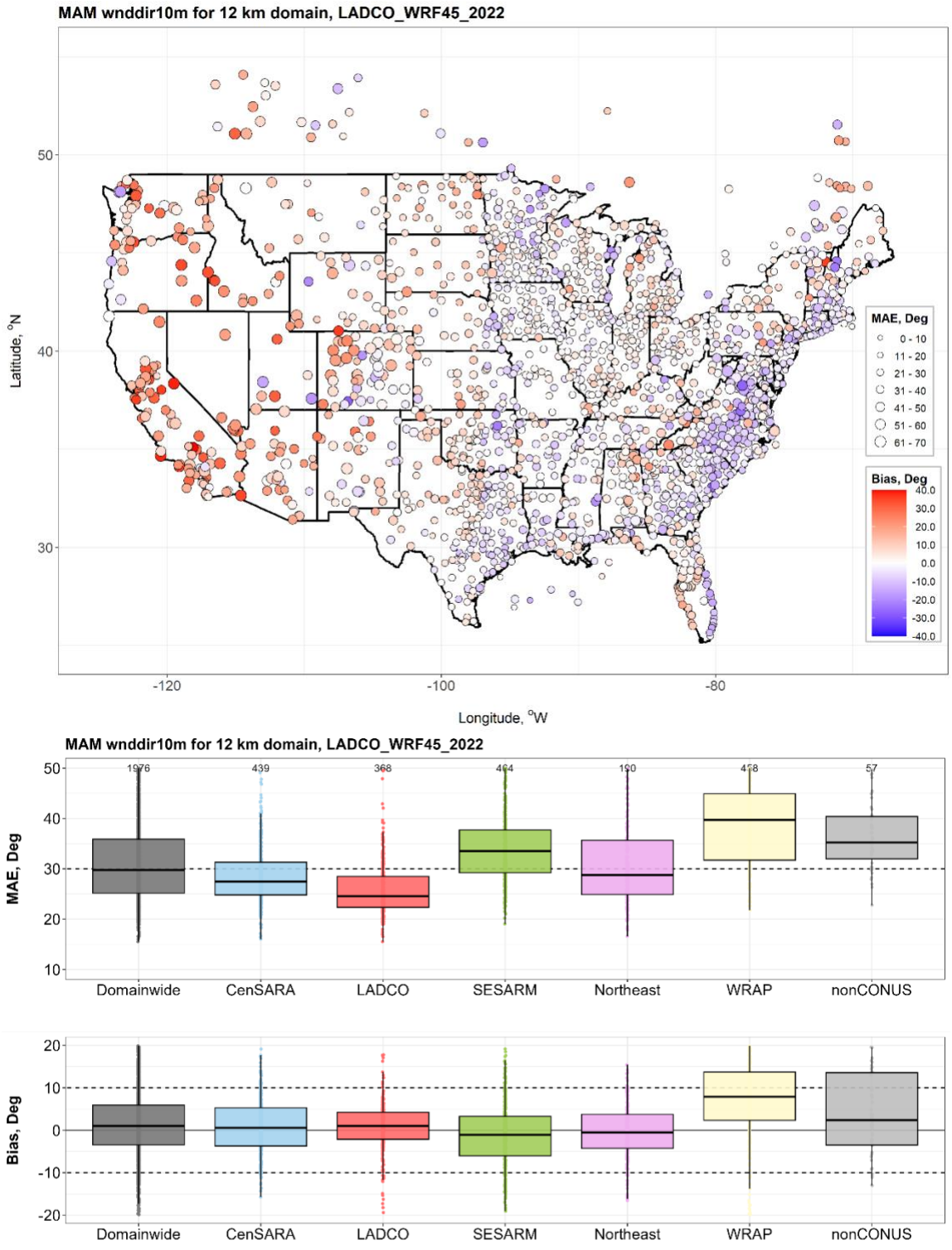

Figure 36. Mean Absolute Errors and Biases for Wind Direction, the 12-km Domain, Spring 2022

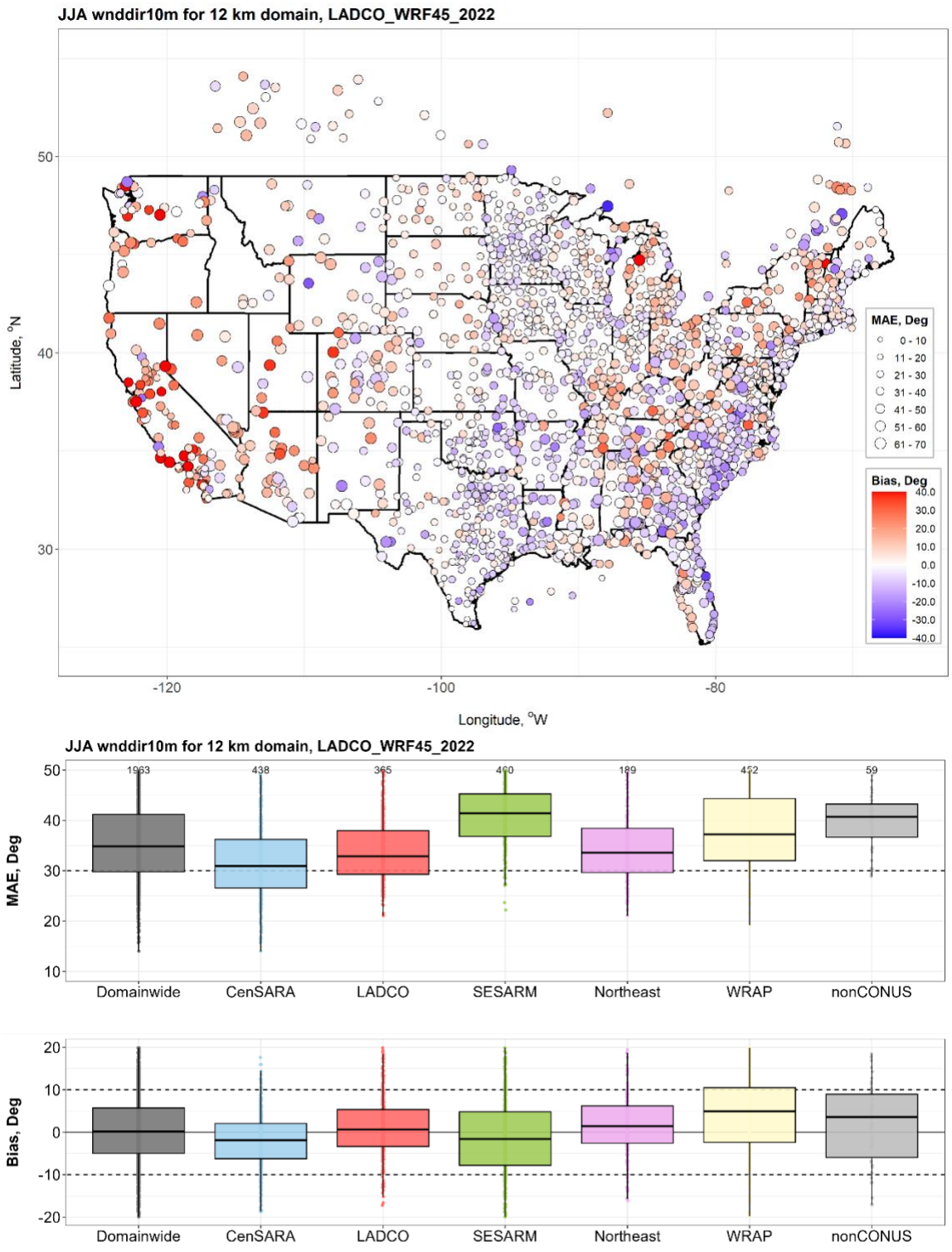

Figure 37. Mean Absolute Errors and Biases for Wind Direction, the 12-km Domain, Summer 2022

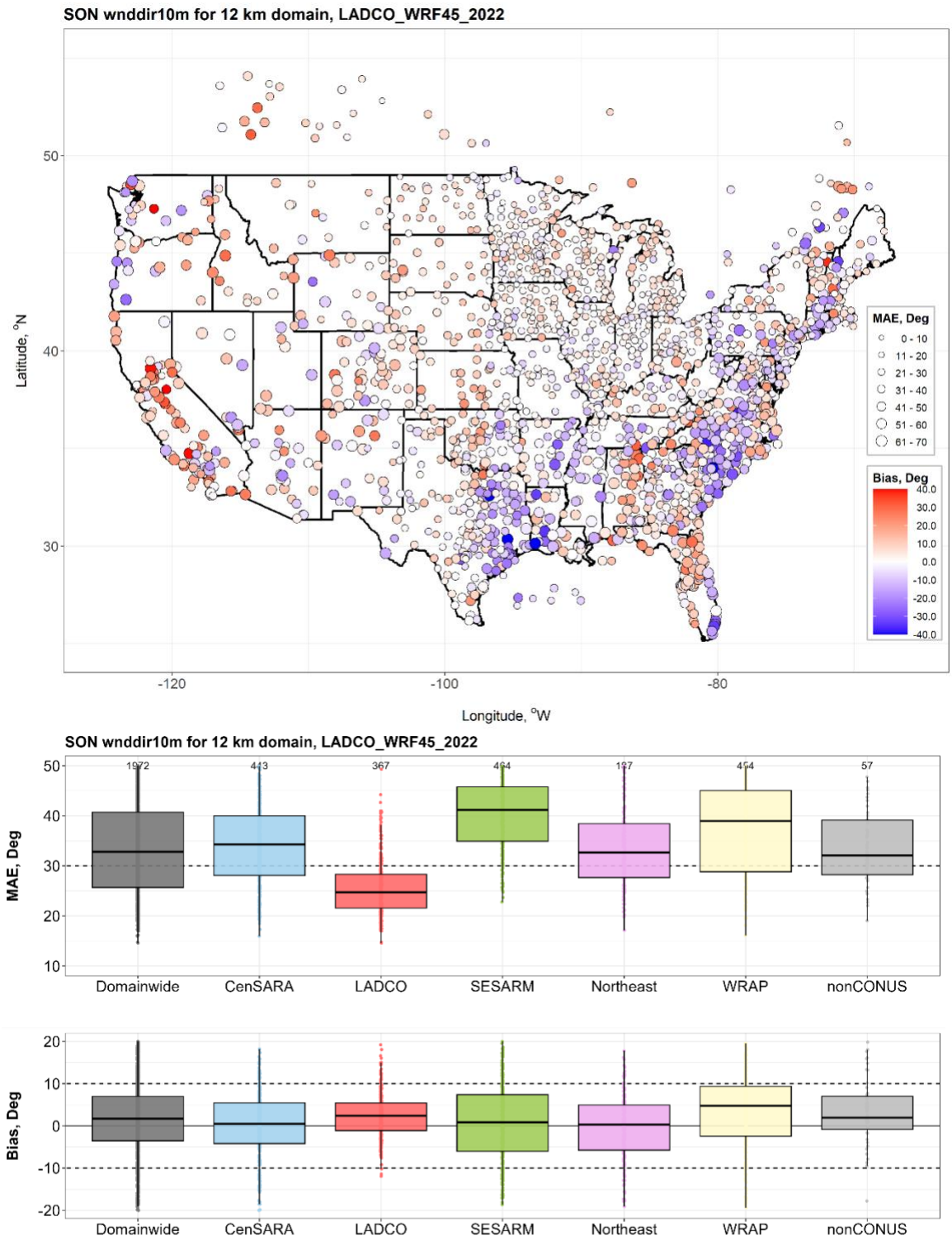

Figure 38. Mean Absolute Errors and Biases for Wind Direction in the 12-km Domain, Fall 2022

A.2 Lake Breeze Analysis Materials

Table 15. Screening results of the lake-breeze events near the Lake Michigan around 2:00-4:00 CST, Summer 2022

Date	NPP/VIIS Surface Reflectance (https://worldview.earthdata.nasa.gov/)	Doppler Radar Reflectivity Composite (https://weather.us/radar-us)	GFS/NCEP/National Weather Service Surface Wind (https://earth.nullschool.net)
4/3/2022	y	n	y
5/4/2022	y	n	y
5/23/2022	y	y	y
6/14/2022	y	y	n
6/23/2022	n	y	y
6/27/2022	n	y	y
6/29/2022	y	y	y
7/3/2022	y	y	y
7/5/2022	y	y	y
7/6/2022	y	n	y
7/7/2022	y	n	y
7/13/2022	y	y	y
7/14/2022	y	y	y
7/25/2022	y	y	
7/26/2022	y	y	y
7/30/2022	y	y	y
7/31/2022	y	y	
8/5/2022	y	y	y
8/9/2022	y	y	y
8/11/2022	y	y	
8/16/2022	y	y	
8/17/2022	y	n	y
8/18/2022	y	y	y
8/21/2022	y	y	
8/22/2022	y	y	y
8/23/2022	y	n	y
8/24/2022	y	y	y
8/26/2022	y	y	y
9/3/2022	y	y	n
9/6/2022	y	y	n
9/7/2022	y	y	y
9/8/2022	y	y	n
9/10/2022	y		y
9/14/2022	y, smoke	y	n

.